Supplementary materials

SiO_2 nanoparticles change colour preference and cause Parkinson's-like behaviour in zebrafish

Xiang Li[1,‡], Bo Liu[2,‡], Xin-Le Li[3,‡], Yi-Xiang Li[1], Ming-Zhu Sun[2], Dong-Yan Chen[3,*], Xin Zhao[2,*], Xi-Zeng Feng[1,*]

[1]State Key Laboratory of Medicinal Chemical Biology, College of Life Science, Nankai University, Tianjin 300071, China.

[2]The Institute of Robotics and Automatic Information Systems, Nankai University, Tianjin 300071, China.

[3]The Key Laboratory of Animal Models and Degenerative Diseases, Department of Physiology, School of Medicine, Nankai University, Tianjin, 300071, China

‡ These authors contributed equally to this work.

Contents

SUPPLEMENTARY METHODS

1. Self-designed video-tracking Software introduction

We utilized self-designed Zebrafish tracking software. Aiming at precise tracking of single adult Zebrafish, the self-organizing background subtraction [1, 2]and blob tracking algorithm[3] which is effective for single target tracking are integrated and implemented. Based on precise moving object (Zebrafish) detection, the blob tracking algorithms use Kalman Filter for Zebrafish location prediction and matching. Our algorithms perform precise, high-throughput and robust tracking which is capable of further behavioral research. To quantify the performance of software, our results are compared with manually labeled trajectories (at the same time stamp concerned about the manually labeled trajectory is sparse) according to **Supplementary Figure S1.** And the tracking error per frame is 0.3567 centimeters and over 90% tracking error is below 0.5 centimeters, according to **Supplementary Figure S2,** in comparison with manual trajectories according to 40-minute test video which covers the possible disturbance in our experiment environment. Moreover, the speed of our software is 5.6869 FPS. Hence, the accuracy and speed of self-designed Zebrafish tracking software is qualified for high-throughput and complex behavioral research.

Besides its accuracy and speed, automated Zebrafish tracking software enjoys indisputable advantages over manual trajectories of trajectory density which stands for more abundant behavior information. Furthermore, based on such precise and dense trajectory, very complex behavior features containing in swimming distance, velocity, stay time, freezing, swimming, rapid movement detection, thigmotaxis, turn

angle and turn angle velocity are quantified and brought into research. Such complex features are capable of quantifying the neurobehavioral parameters such as locomotive activities and color preference for further analysis.

Among all the features, distance, stay time and velocity are calculated directly from trajectories. The locomotive status, based on instantaneous velocity, is classified into three categories, freezing for velocity less than 1 cm/s, swimming for velocity between 1 cm/s and 10 cm/s and rapid movement for velocity more than 10cm/s. The thigmotaxis is defined as the distance of detected Zebrafish to nearest wall of container during 3minuts test. The turning angle and turn angle velocity are calculated through intersection angle between continuous two moving vectors

$$\begin{aligned}\overrightarrow{V_t} &= (x_t - x_{t-1}, y_t - y_{t-1}) \\ \overrightarrow{V_{t+1}} &= (x_{t+1} - x_t, y_{t+1} - y_t) \\ \cos(A_t) &= \frac{\overrightarrow{V_t} \bullet \overrightarrow{V_{t+1}}}{\left|\overrightarrow{V_t}\right| \bullet \left|\overrightarrow{V_{t+1}}\right|}\end{aligned} \quad . \qquad (1.1)$$

Amongst, (x_t, y_t) is coordinate of Zebrafish at time t and A_t is turning angle. The instantaneous features are used for visualization and they are averaged for statistically analyzed. On the other hand, the comparison between average features in left and right in two colored compartments in CPP serves as direct way to quantify the SiO_2-NPs influence on Zebrafish's color preference and locomotive activities.

2. Clustering Analysis:

In clustering, the average features are compared with control group by subtracting the mean of control group and dividing the standard variation of control group to convert the average features to standard deviation. As to comparison features, they are

defined as

$$F_{comp} = \frac{F_{left}}{F_{left} + F_{right}} \tag{1.2}$$

Naturally, the vector containing in average features and comparison features represents the behavioral characteristic of single Zebrafish. Then, based on feature vector, the hierarchical clustering algorithms based on Euclidean distance (all features are standardized) and average linkage is used on Zebrafish behavioral data.

SUPPLEMENTARY TABLE

Particles	Mean size(nm)	Zeta potential(mv)
15nm-300μg/mL SiO_2	290.9nm	-11.35
-1000μg/mL SiO_2	837.4nm	-12.82
50nm-300μg/mL SiO_2	1024.1nm	-12.84
-1000μg/mL SiO_2	1781.4nm	-14.39

Supplementary Table S1: Particles mean size and zeta potential of SiO_2-NPs of different size and concentration in standard tank water.

Results of DLS demonstrated that the size and charge of SiO_2-NPs dissolved in standard tank water (KCl 0.05 g/L, $NaHCO_3$ 0.025 g/L, NaCl 3.5 g/L and $CaCl_2$ 0.1 g/L, pH 7.0-7.2). Agglomeration size increases when concentration is higher and size of silica bigger. Likewise, the absolute value of zeta potential. It is obviously presented in table that charge value of SiO_2-NPs agglomeration in standard tank water is dependent on the size of the agglomeration, that is, as the concentration increased mean size of the SiO_2-NPs agglomeration enlarged and the charge of the agglomeration is more negative.

SUPPLEMENTARY FIGURE

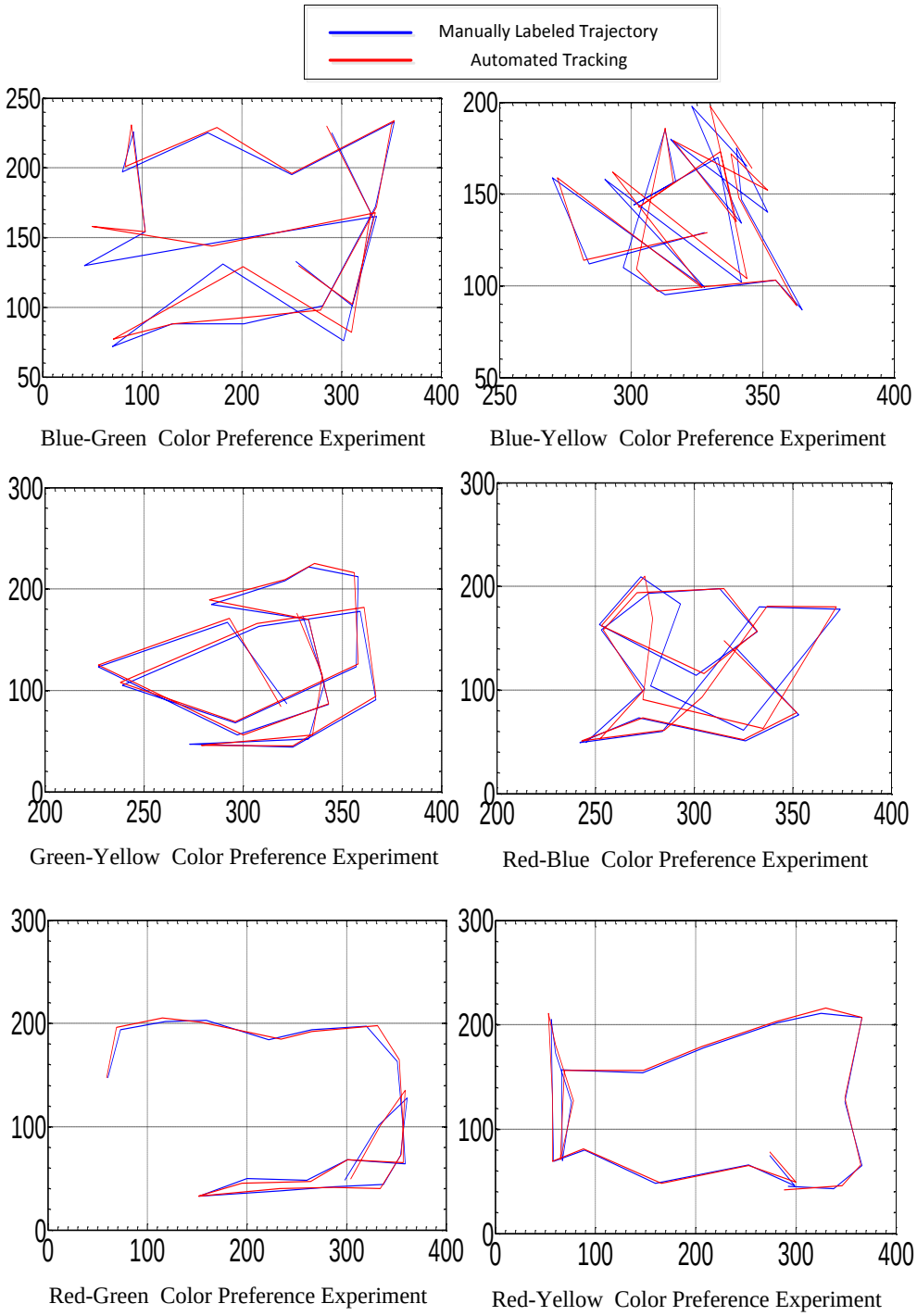

Supplementary Figure S1: Comparison of automated and manual trajectory

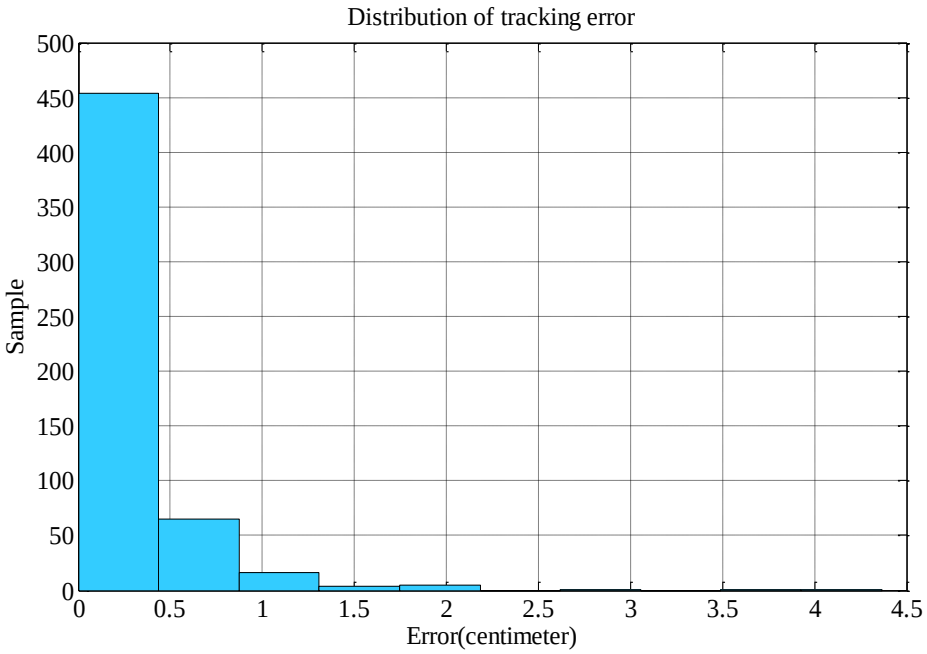

Supplementary Figure S2: Histogram of tracking error per frame

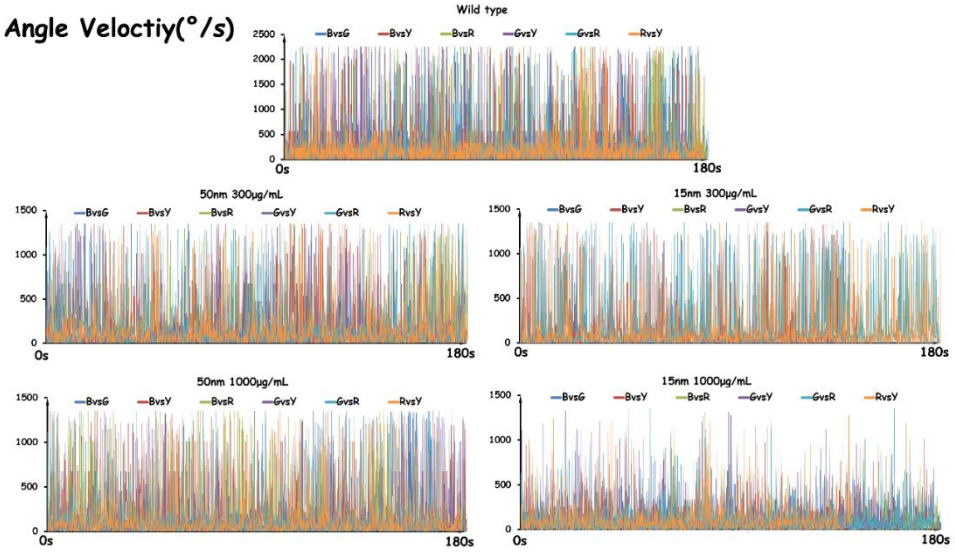

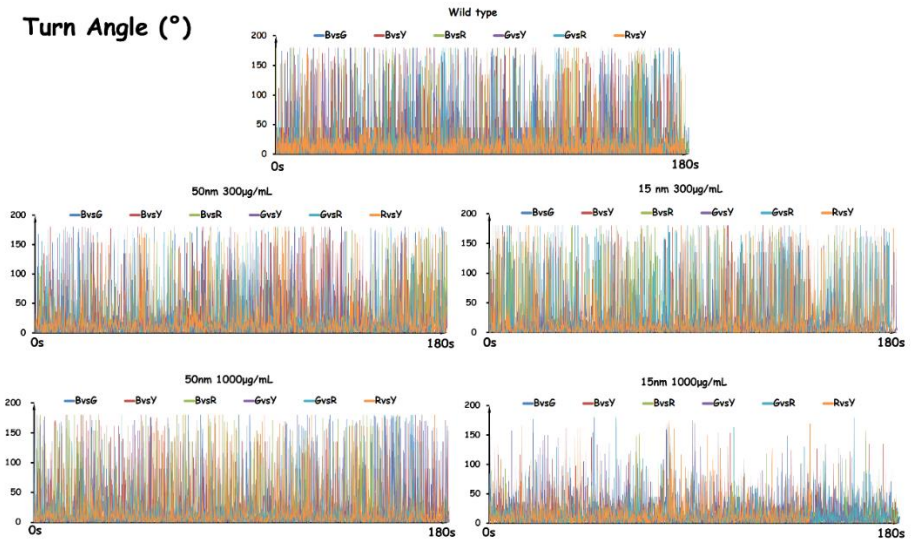

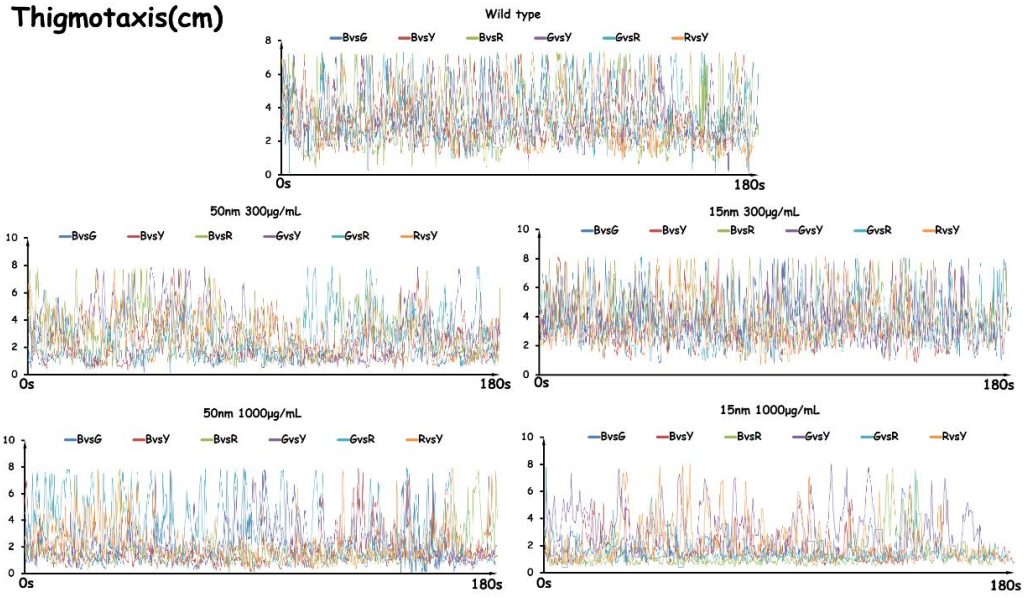

Supplementary Figure S3： Real time sequence diagram of locomotion and color preference parameters extracted from 18-min (six color combination with 3-min every combination) video tracking of SiO_2-NPs treated zebrafish.

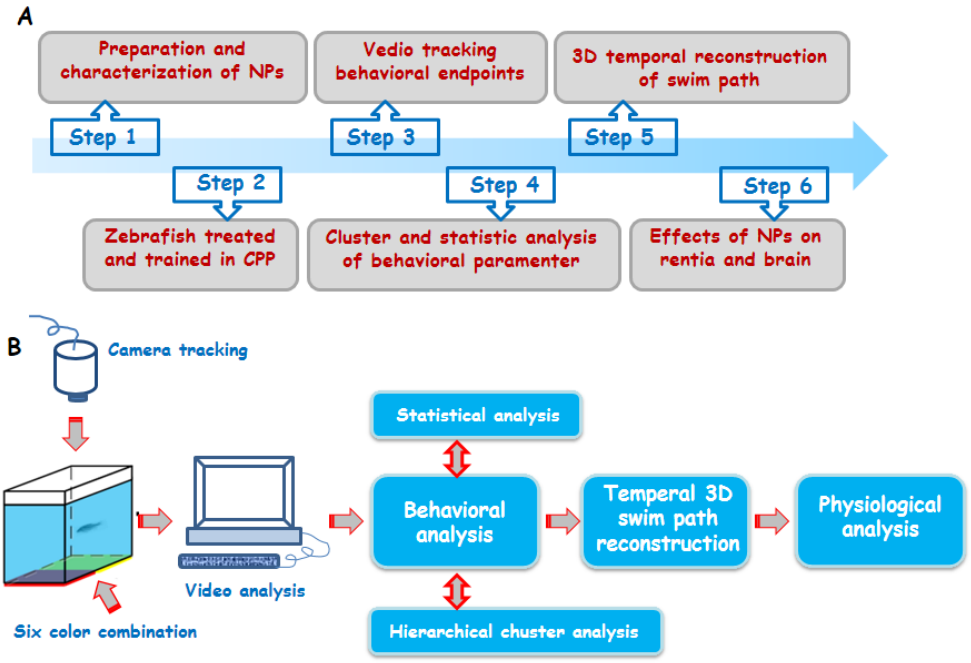

Supplementary Figure S4: Flowchart illustrating the experimental strategy of this research. The illustration **(A)** includes SiO_2-NPs distribution and diameter detection by DLS (Dynamic Light Scattering) in standard tank water (Step 1). Zebrafish were trained in CPP tank and dosed in habitual tanks for seven days before tested (Step 2). During the process of test, 9 behavioral endpoints as well as the swimming path of zebrafish were recorded by video (Step 3). Subsequently, Clustering and statistical analysis were conducted across all the behavioral parameters and experimental treatments in order to discover potential size and concentration effect of SiO_2-NPs over neural behavior of zebrafish (Step 4). These effect induced by SiO_2-NPs were reconfirmed using the 3D spatiotemporal swim path reconstructions (Step 5). All data were integrated into conclusion concerning the effects of SiO_2-NPs on zebrafish. Physiological analysis were performed to

detect the effect of SiO_2-NPs in different size and concentration on the retina and brain (Step 6). **(B)** Standard procedure of color preference test in CPP tank. Initially, trained wild-type zebrafish were tested in CPP tank with six color combination in the bottom, and for each color combination zebrafish were tested in 3 minutes, which were recorded by video. Animal behavior was automatically observed and one camera recorded videos for automated analysis in self-designed software for zebrfish tracking. Raw data obtained from tracking software were analyzed via Hierarchical cluster and statistics. For spatiotemporal reconstruction, track data for each subject was exported, processed and visualized in a 3D scatter plot with Rapid Miner 5.0.

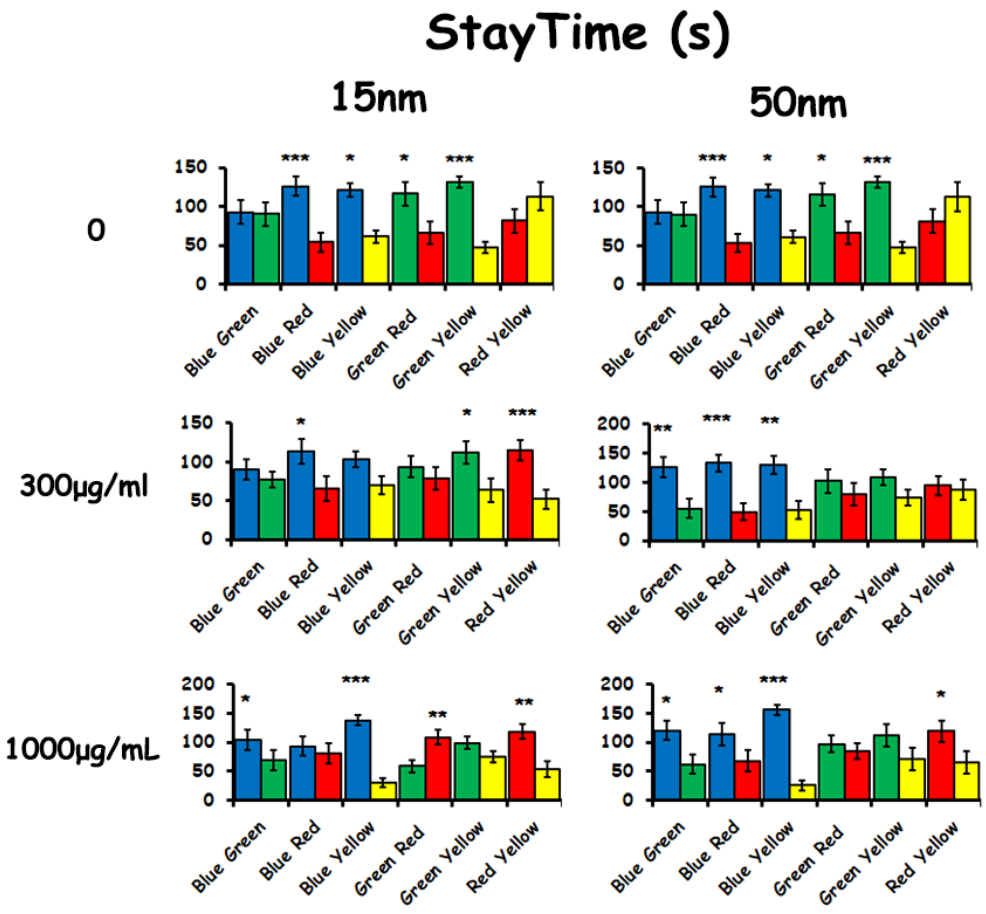

Supplementary Figure S5 (A). Total time spent in each compartment with six different color combinations located within the place preference apparatus. Data represents mean± SEM of n = 12 zebrafish. * p < 0.05, ** p < 0.01, ***p < 0.001.

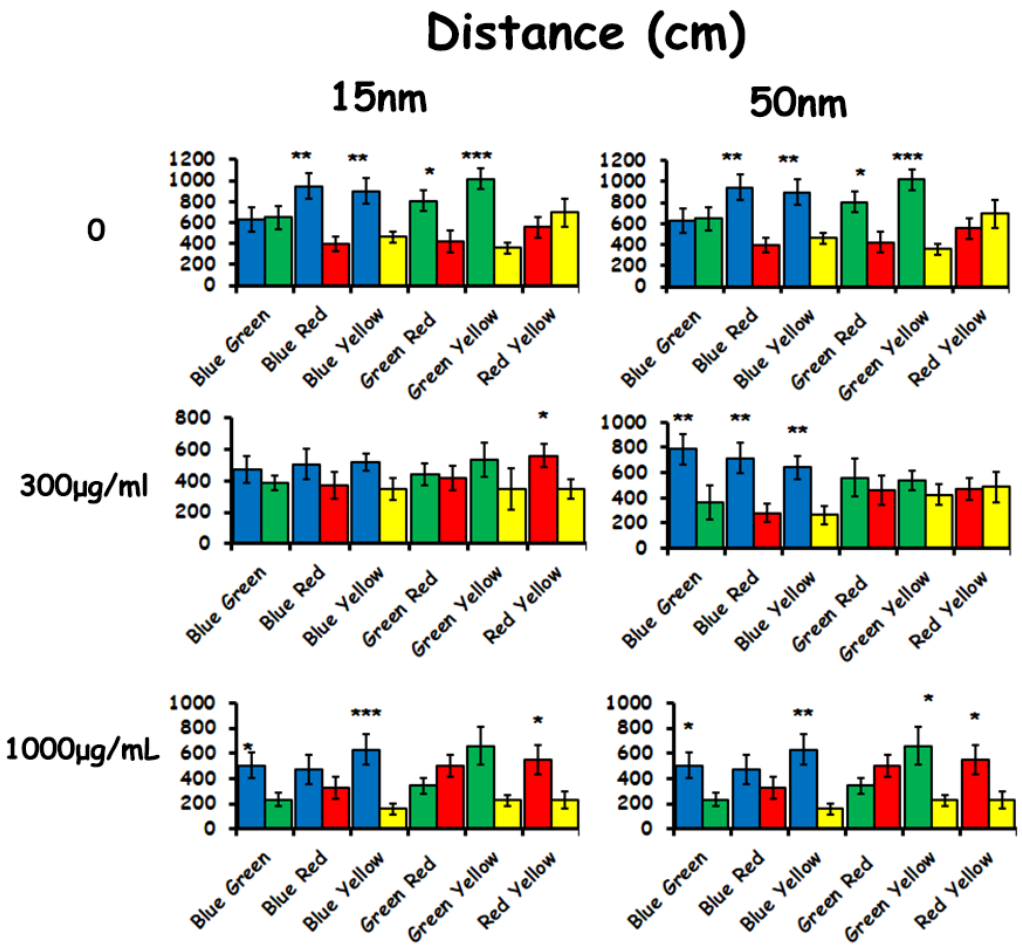

Supplementary Figure S5 (B). Total Distance in each compartment with six different color combinations located within the place preference apparatus. Data represents mean± SEM of n = 12 zebrafish. * p < 0.05, ** p < 0.01, ***p < 0.001.

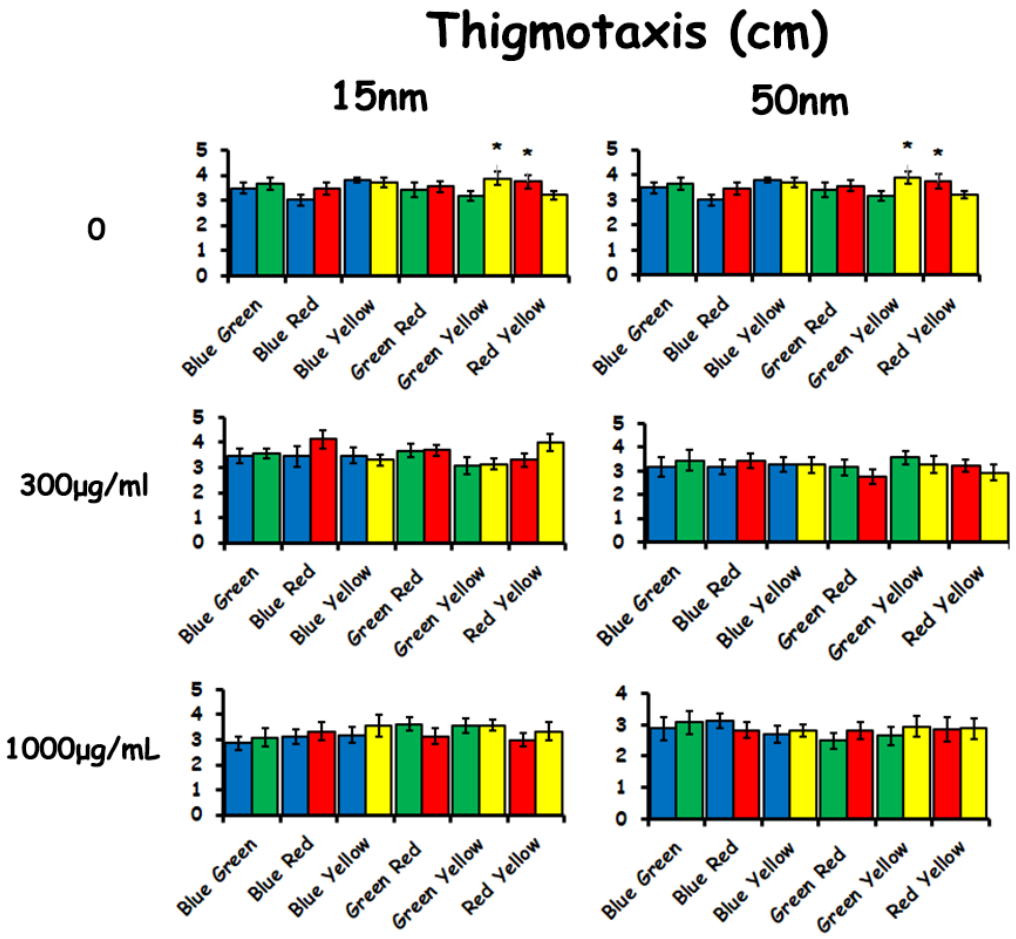

Supplementary Figure S5 (C). Thigmotaxis in each compartment with six different color combinations located within the place preference apparatus. Data represents mean± SEM of n = 12 zebrafish. * p < 0.05, ** p < 0.01, ***p < 0.001.

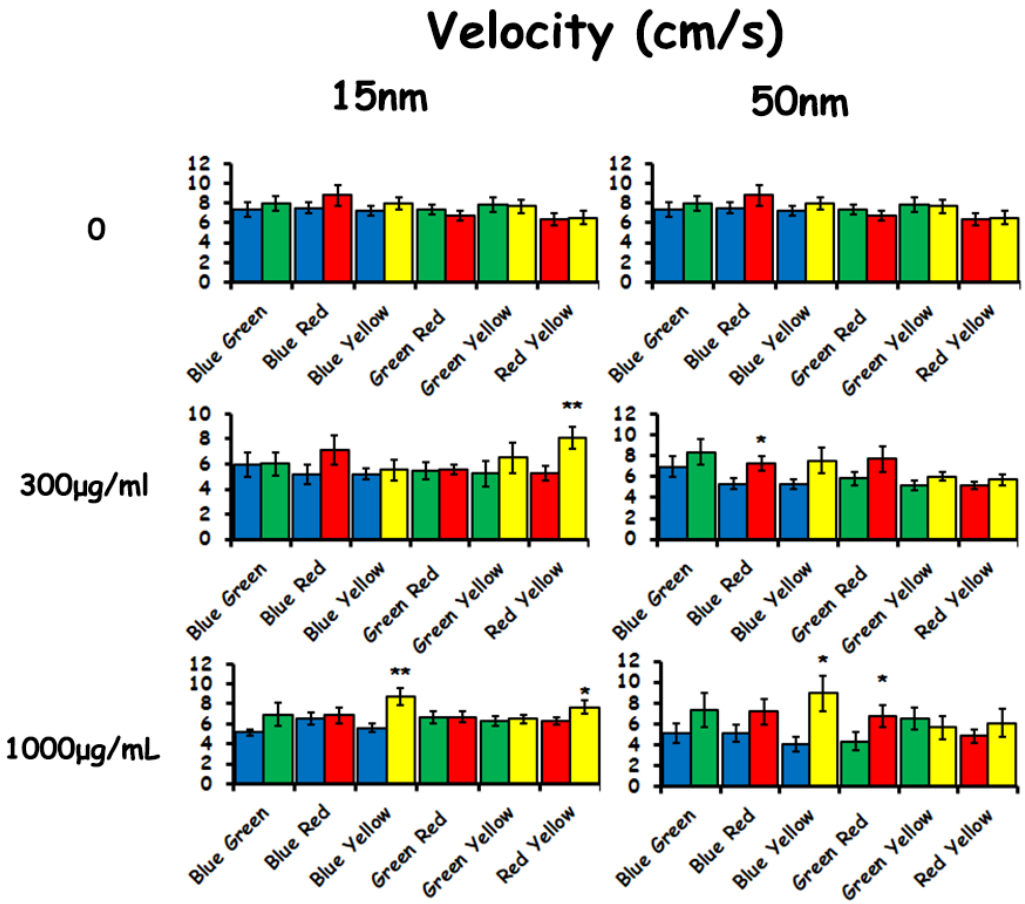

Supplementary Figure S5 (D). Mean velocity in each compartment with six different color combinations located within the place preference apparatus. Data represents mean± SEM of n = 12 zebrafish. * p < 0.05, ** p < 0.01, ***p < 0.001.

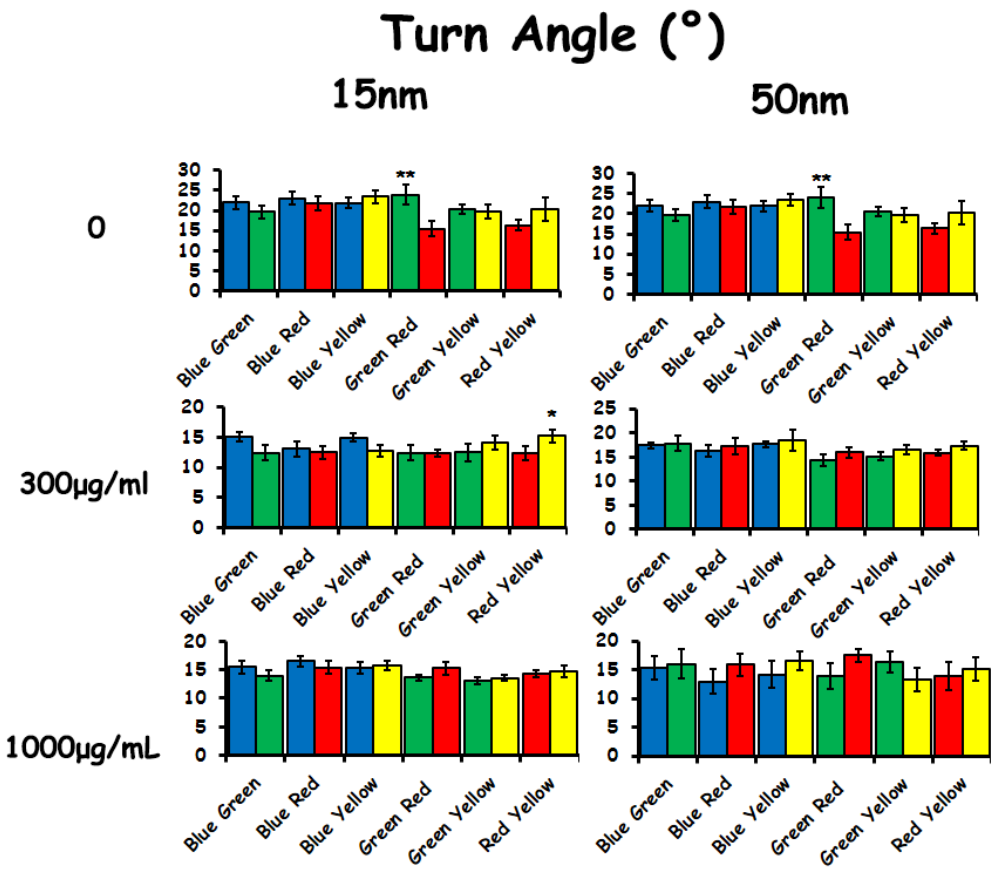

Supplementary Figure S5 (E). Mean Turn Angle in each compartment with six different color combinations located within the place preference apparatus. Data represents mean± SEM of n = 12 zebrafish. * p < 0.05, ** p < 0.01, ***p < 0.001.

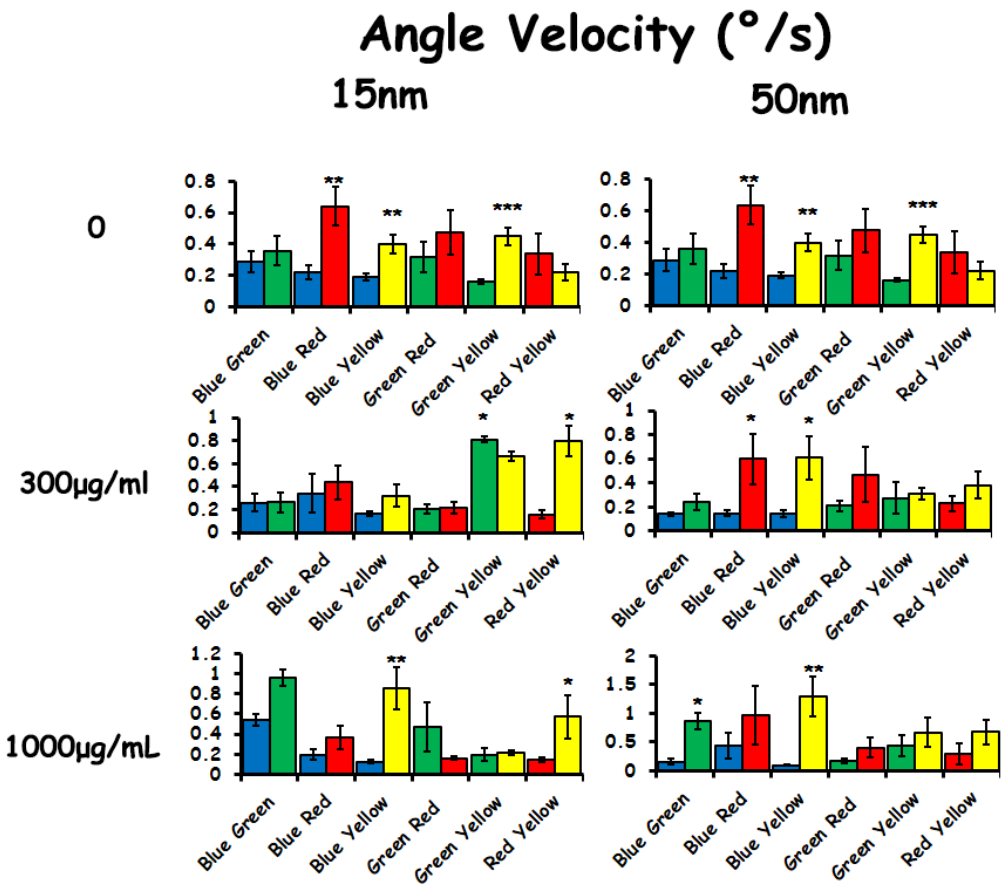

Supplementary Figure S5 (F). Mean Angle Velocity in each compartment with six different color combinations located within the place preference apparatus. Data represents mean± SEM of n = 12 zebrafish. * p < 0.05, ** p < 0.01, ***p < 0.001.

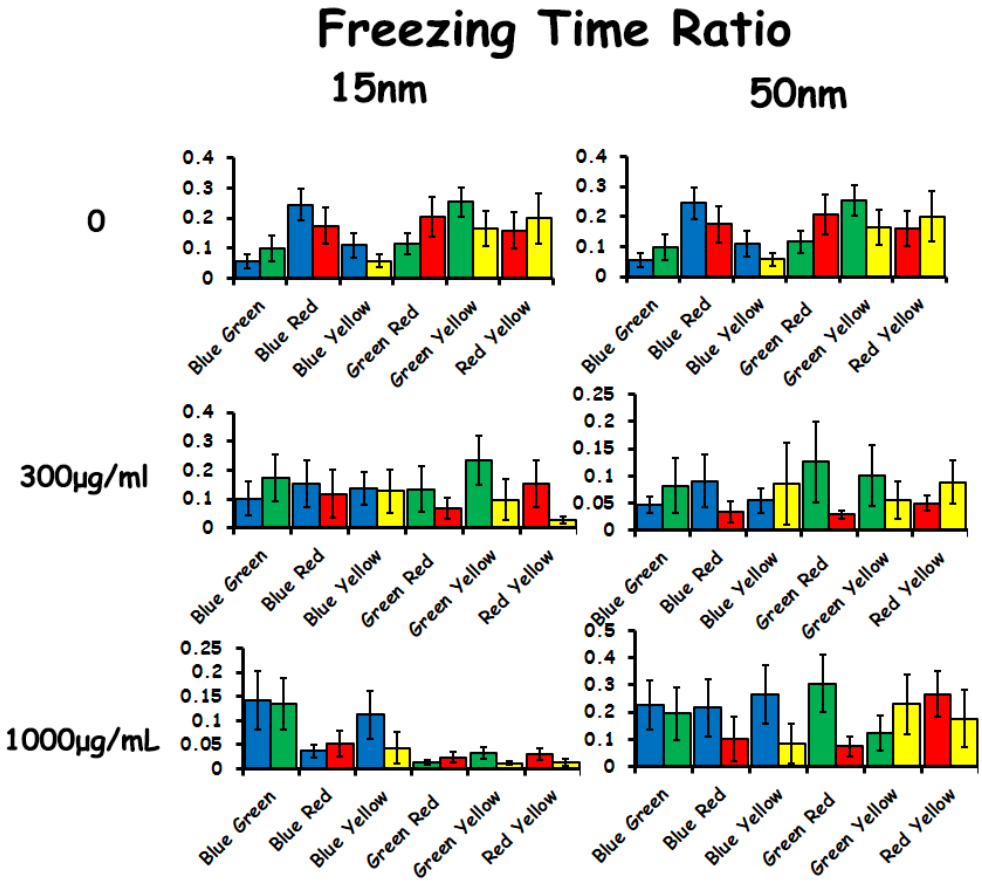

Supplementary Figure S5 (G). Freezing Time Raito in each compartment with six different color combinations located within the place preference apparatus. Data represents mean± SEM of n = 12 zebrafish. * p < 0.05, ** p < 0.01, ***p < 0.001.

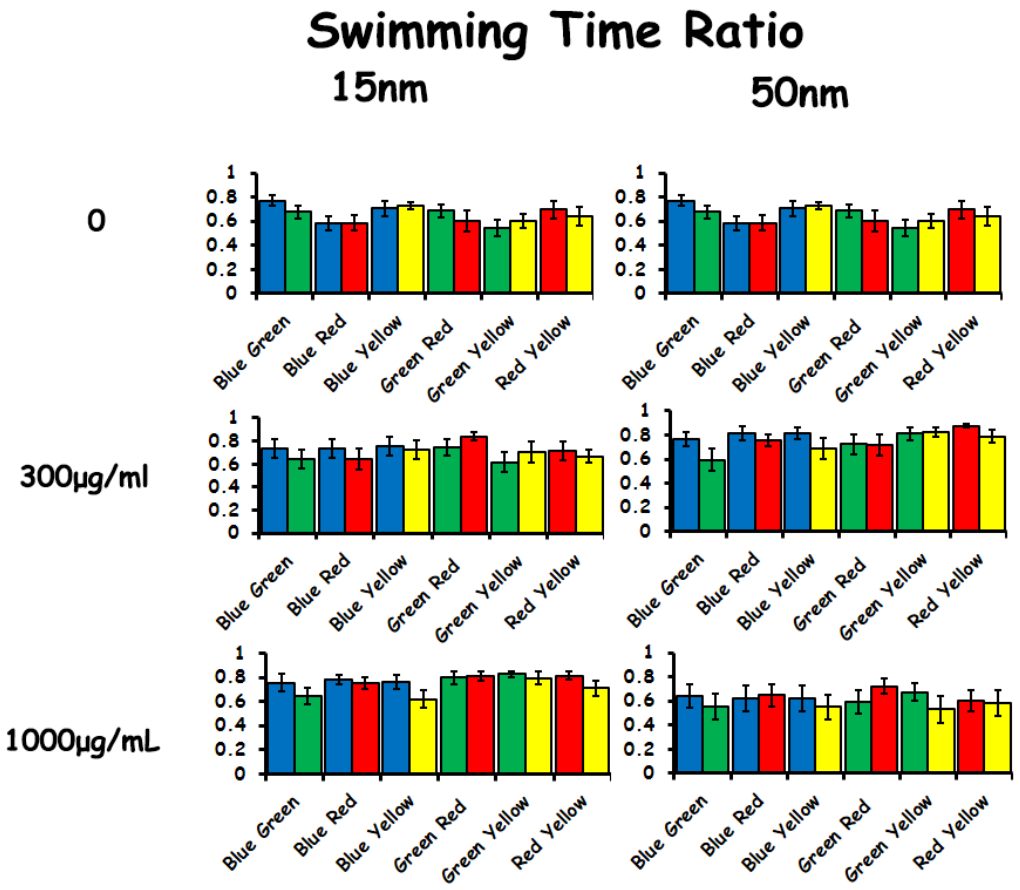

Supplementary Figure S5 (H). Swimming Time Ratio in each compartment with six different color combinations located within the place preference apparatus. Data represents mean± SEM of n = 12 zebrafish. * p < 0.05, ** p < 0.01, ***p < 0.001.

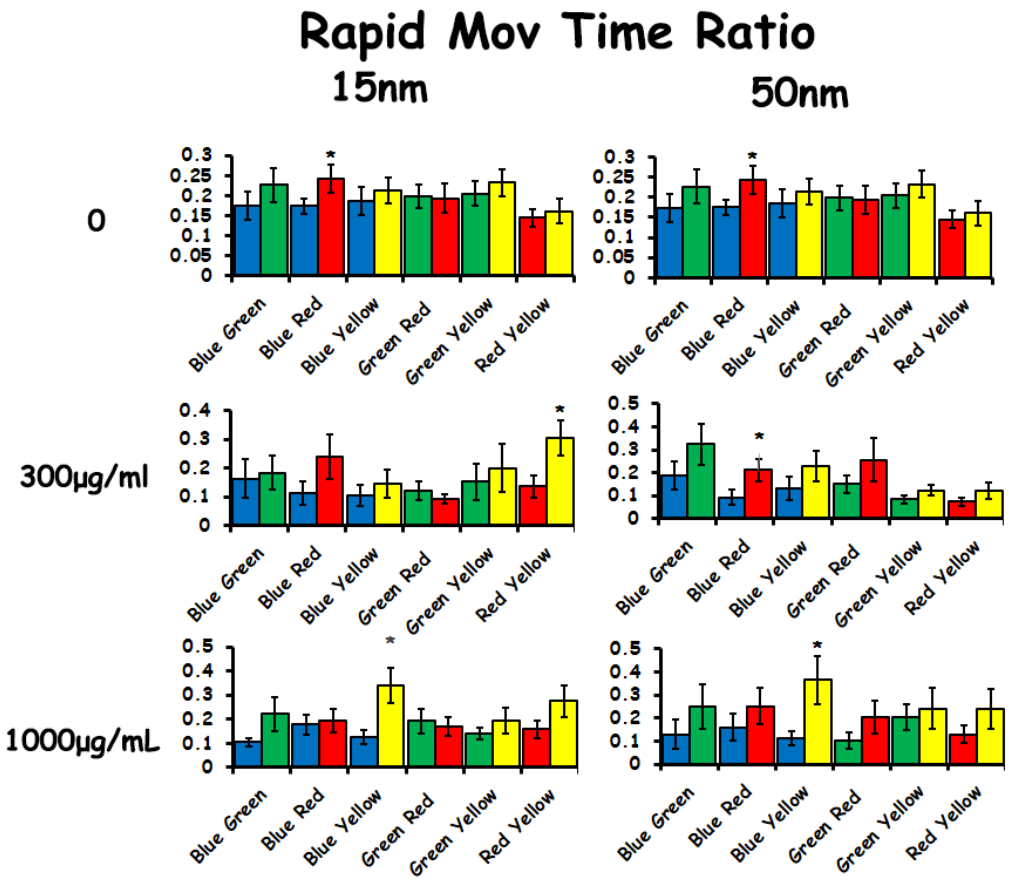

Supplementary Figure S5 (I). Rapid Movement Time Ratio in each compartment with six different color combinations located within the place preference apparatus. Data represents mean± SEM of n = 12 zebrafish. * p < 0.05, ** p < 0.01, ***p < 0.001.

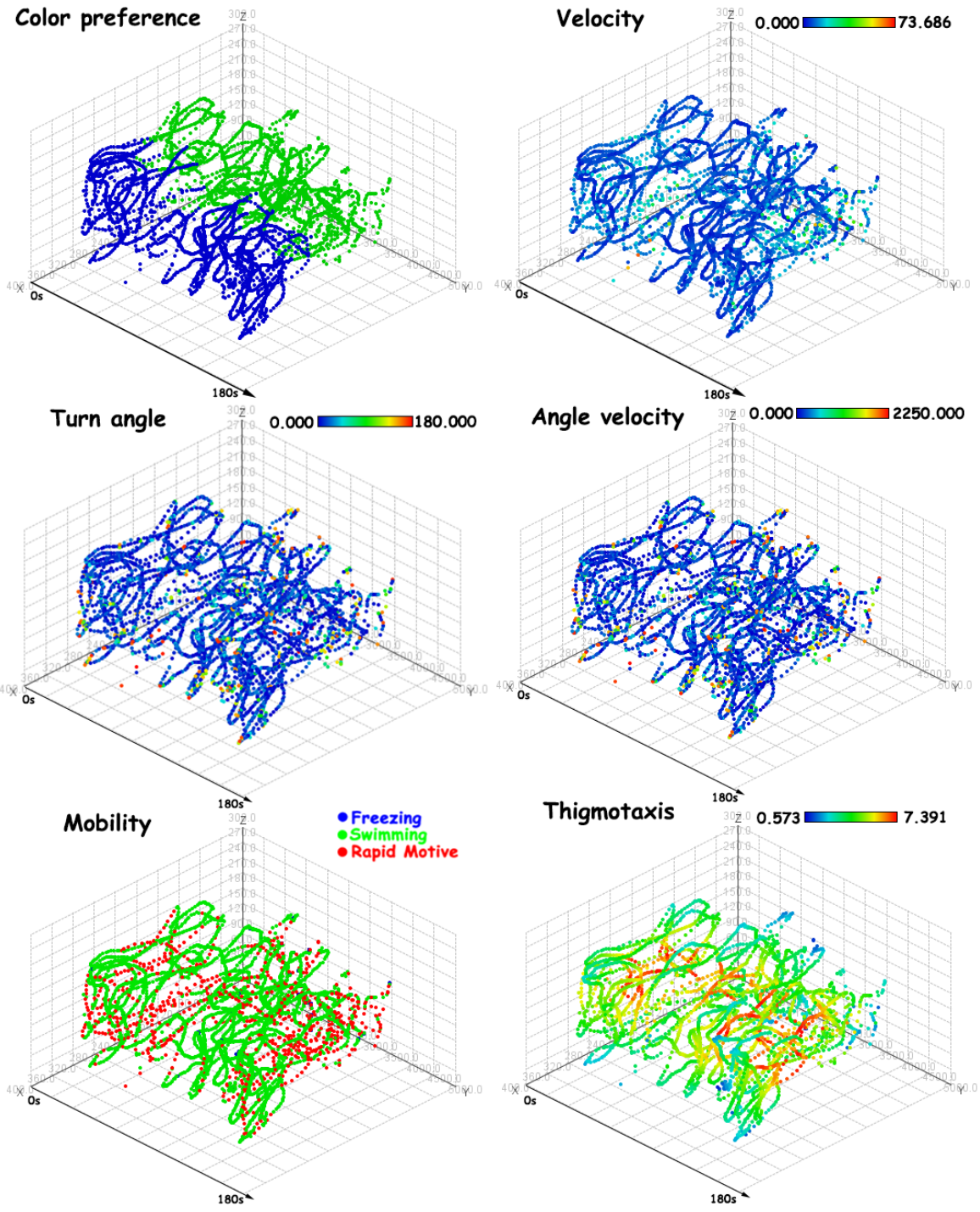

Supplementary Figure S6 (A): wild type

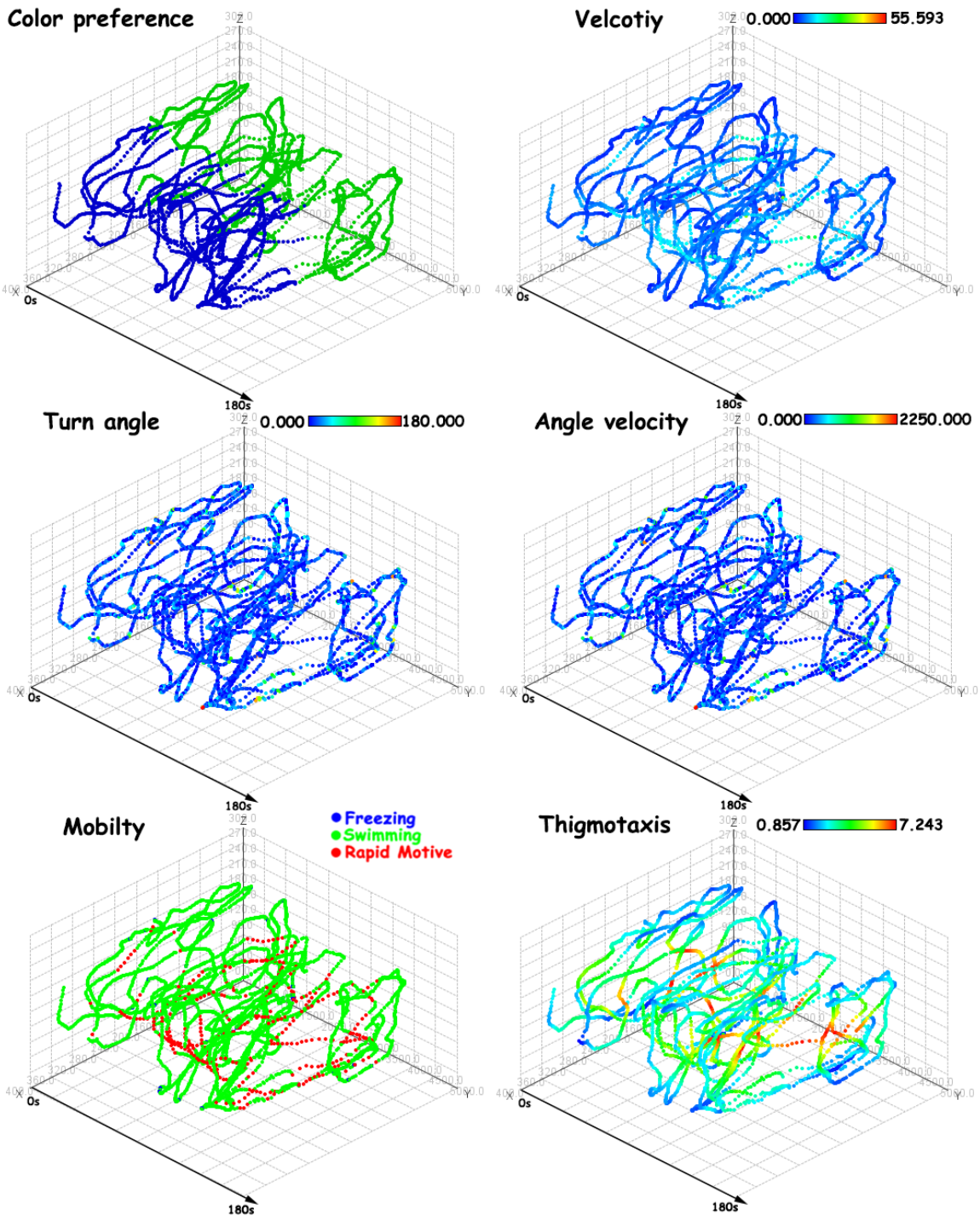

Supplementary Figure S6 (B): 50 nm 300µg/mL

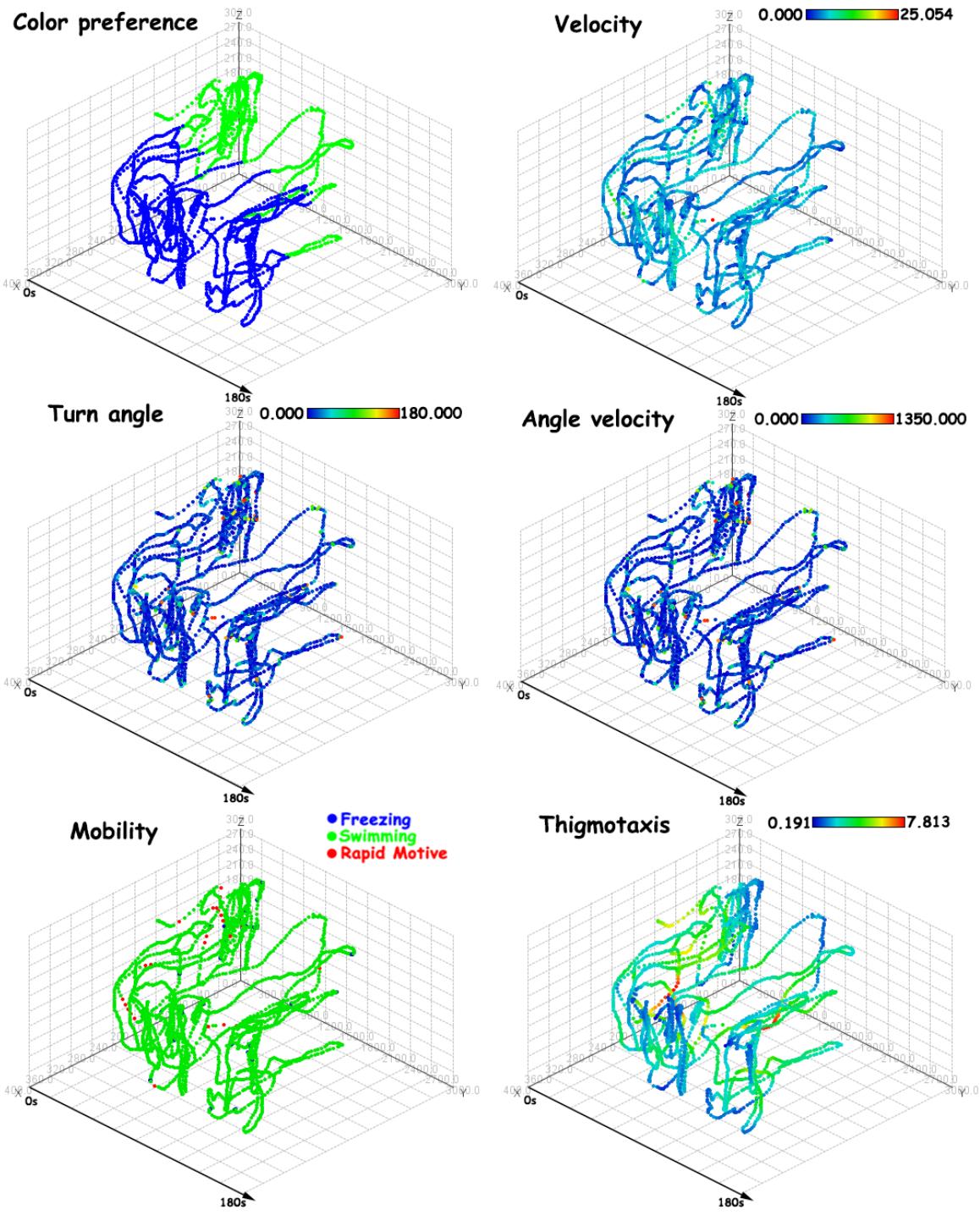

Supplementary Figure S6 (C): 50 nm 1000µg/mL

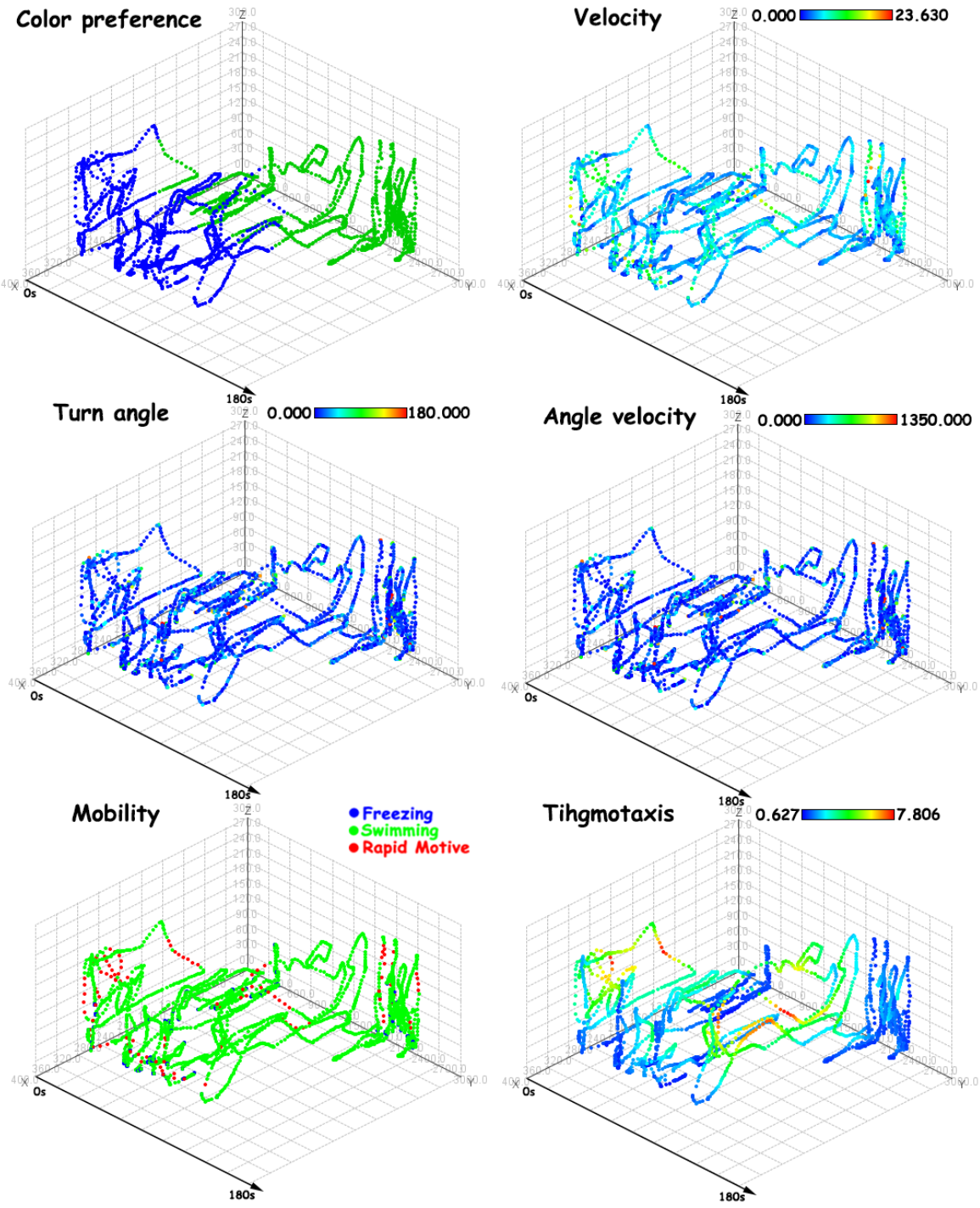

Supplementary Figure S6 (D): 15 nm 300µg/mL

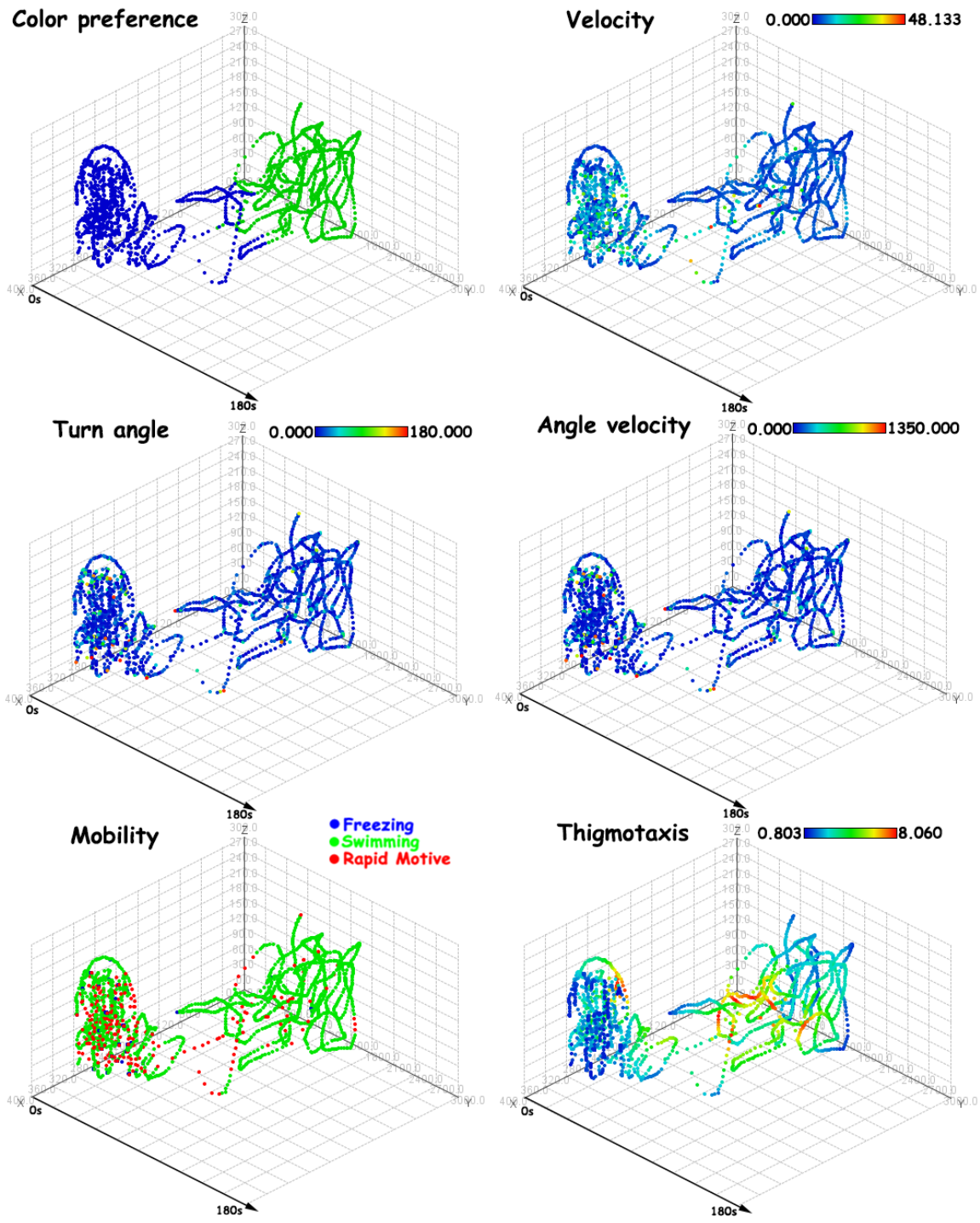

Supplementary Figure S6 (E): 15 nm 1000µg/mL

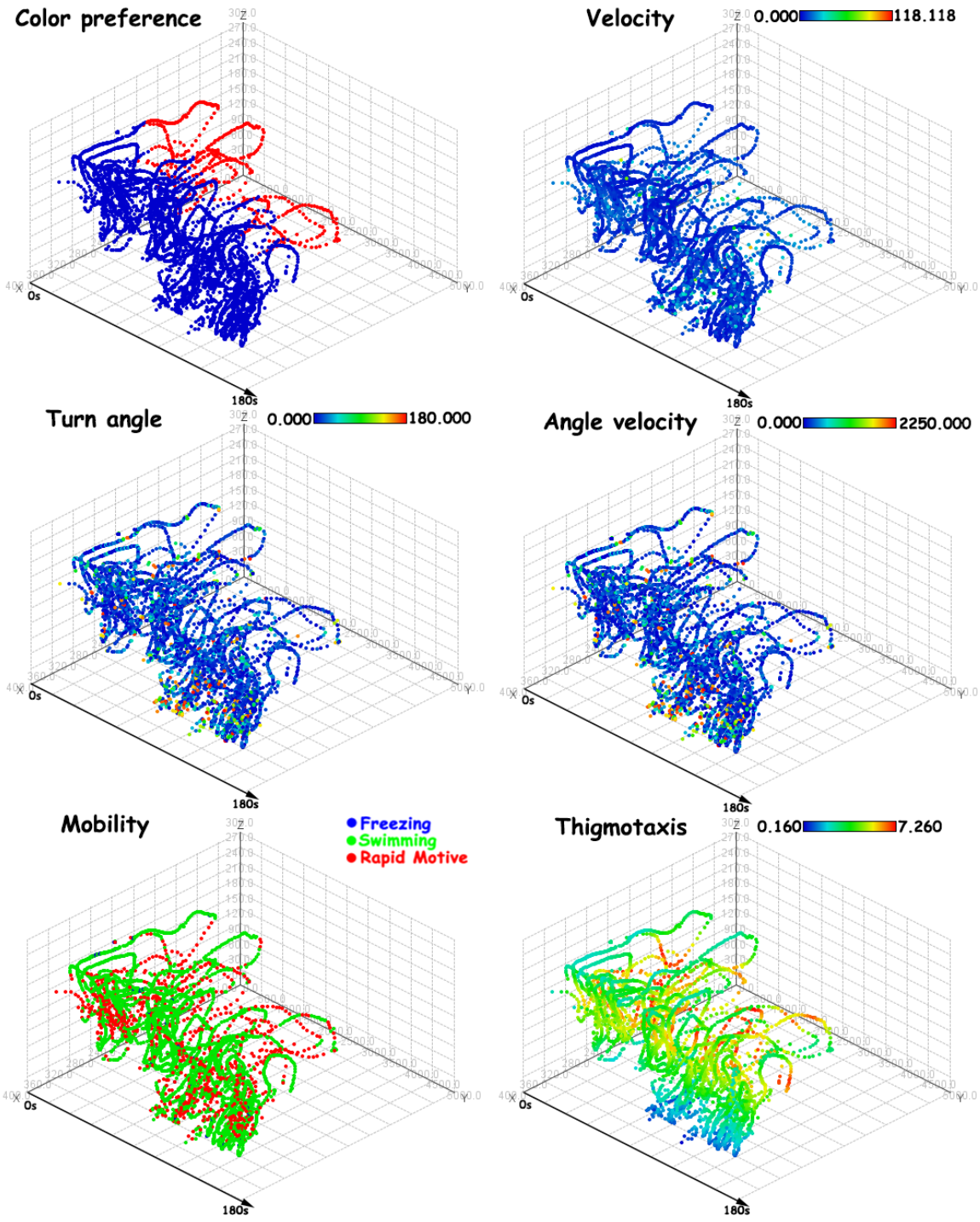

Supplementary Figure S7 (A): Wild type

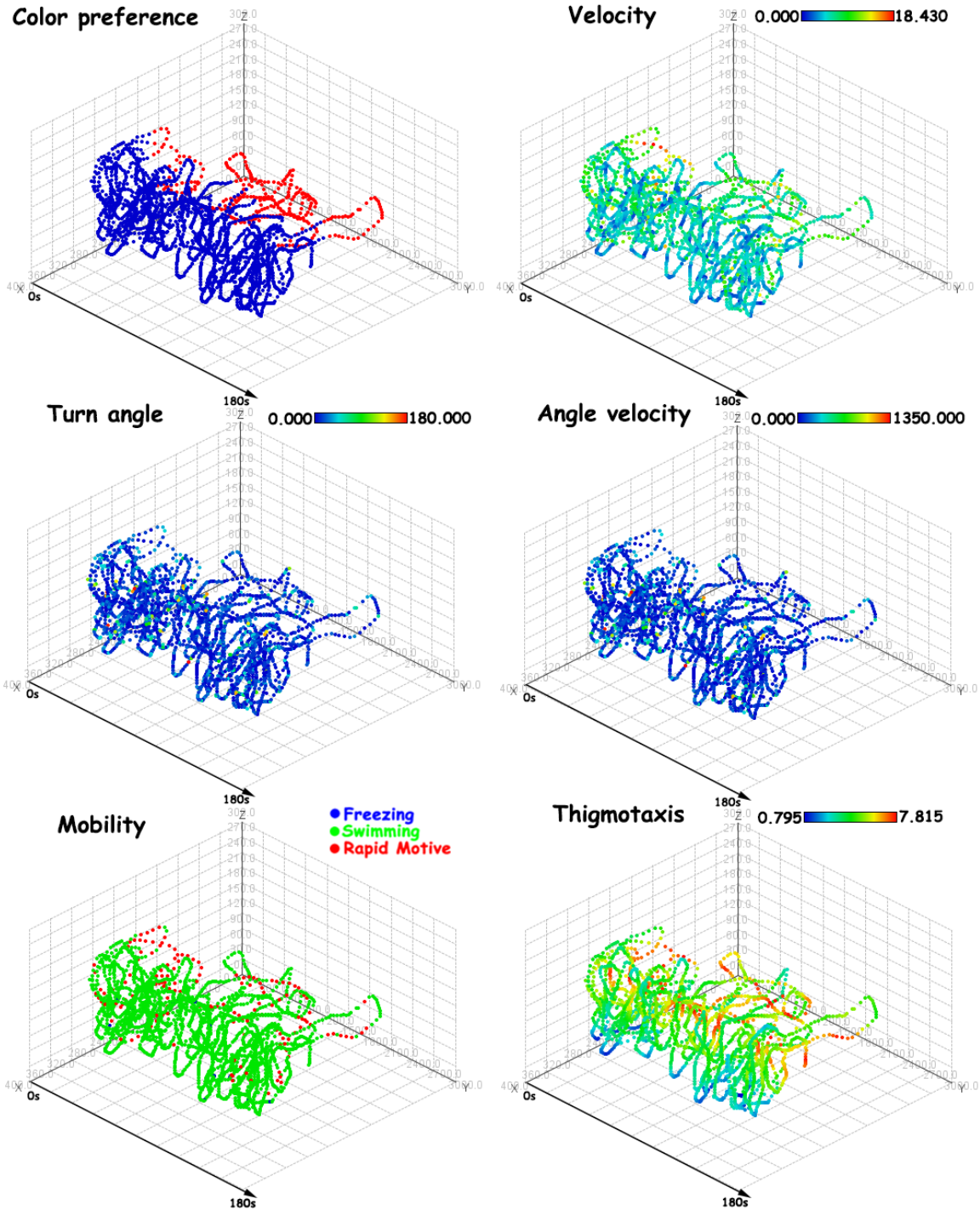

Supplementary Figure S7 (B): 50 nm 300µg/mL

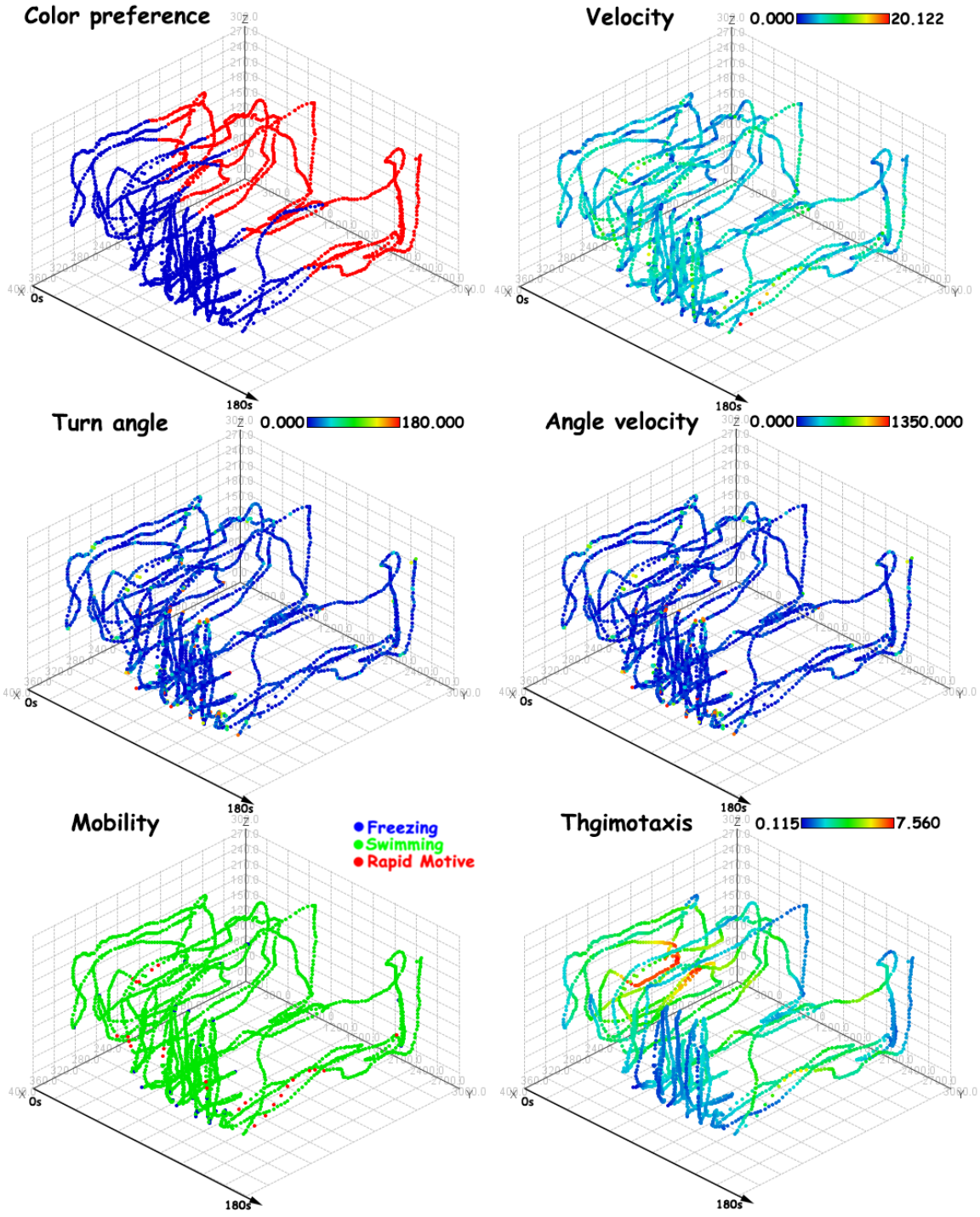

Supplementary Figure S7 (C): 50 nm 1000µg/mL

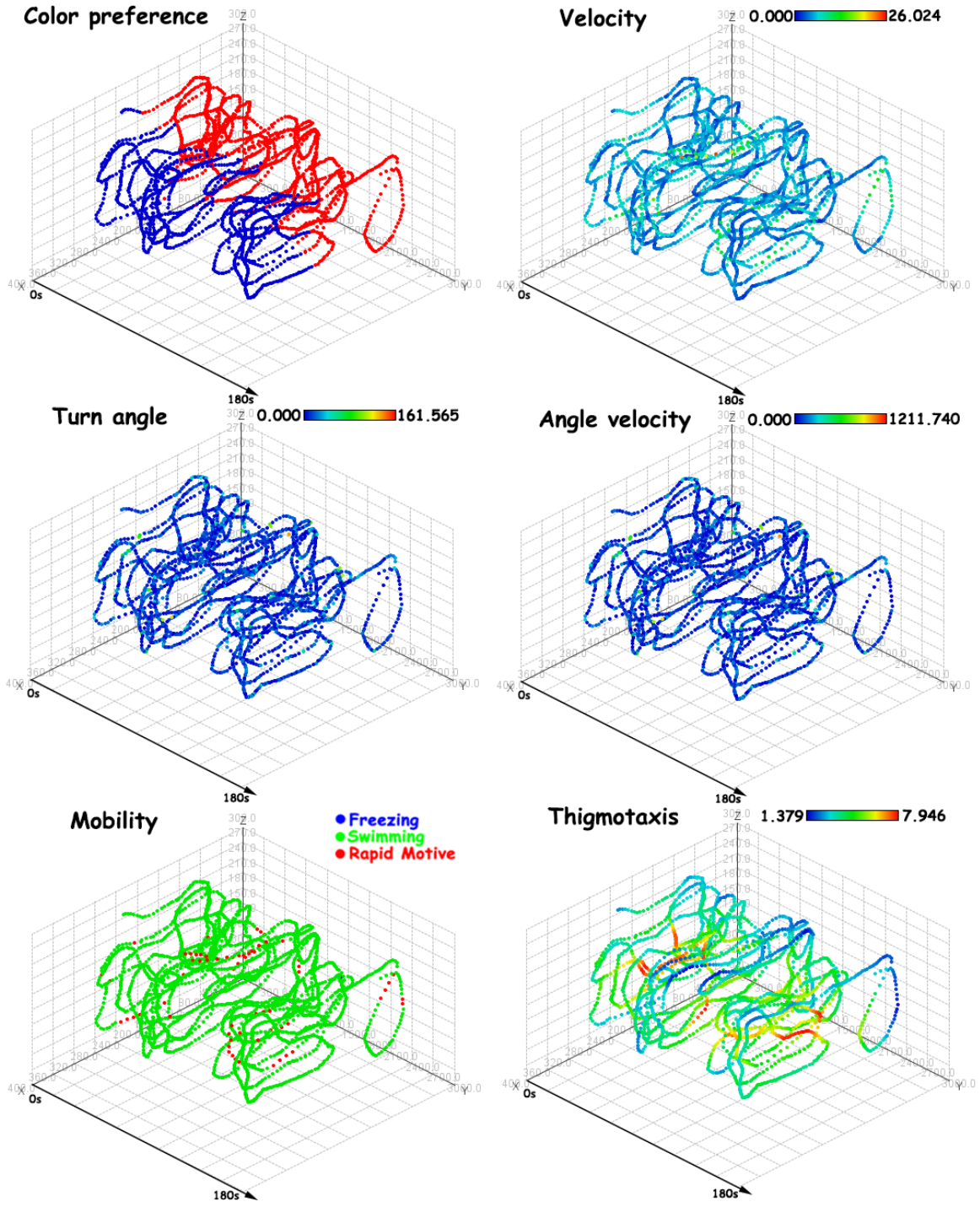

Supplementary Figure S7 (D): 15nm 300μg/mL

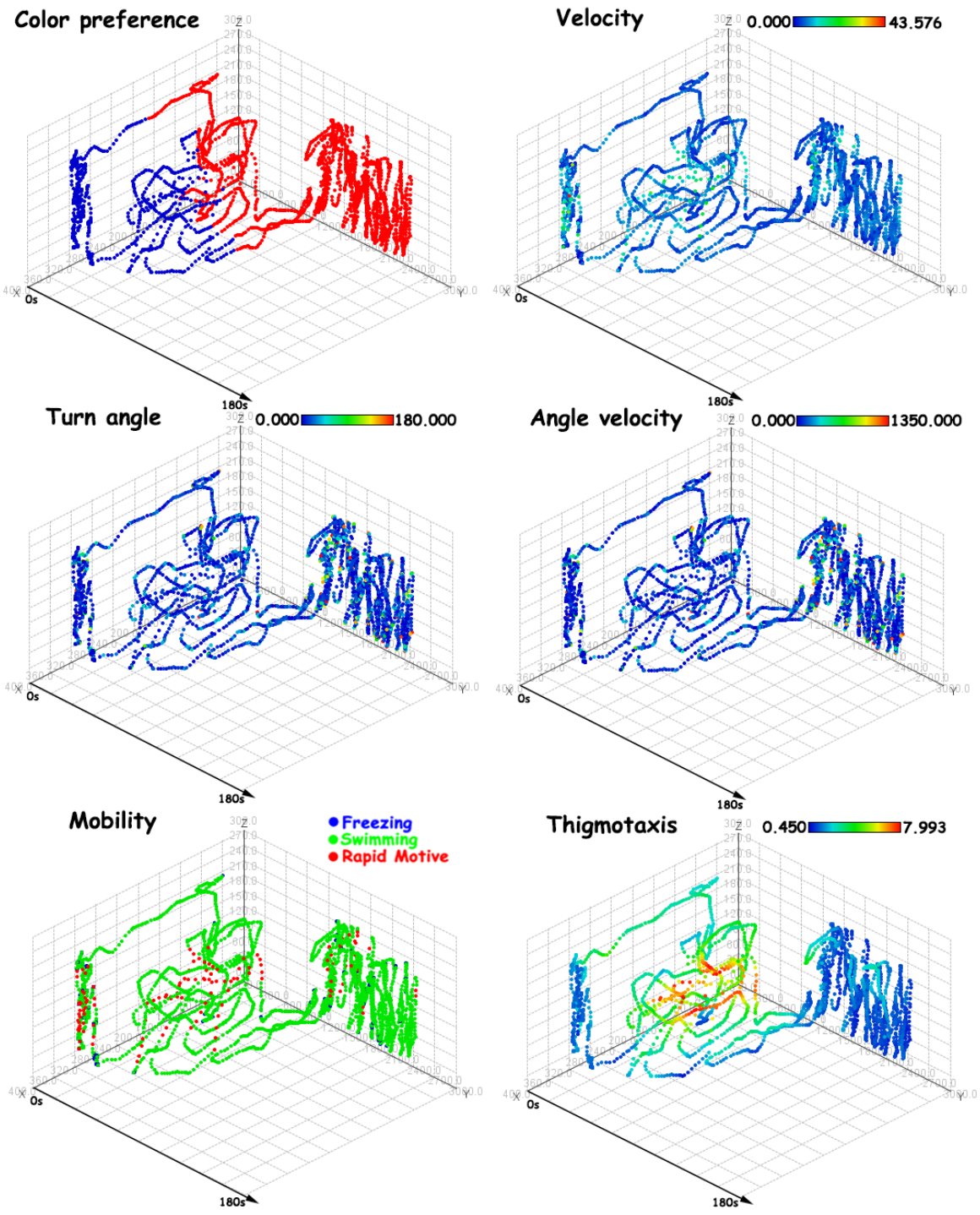

Supplementary Figure S7 (E): 15 nm 1000µg/mL

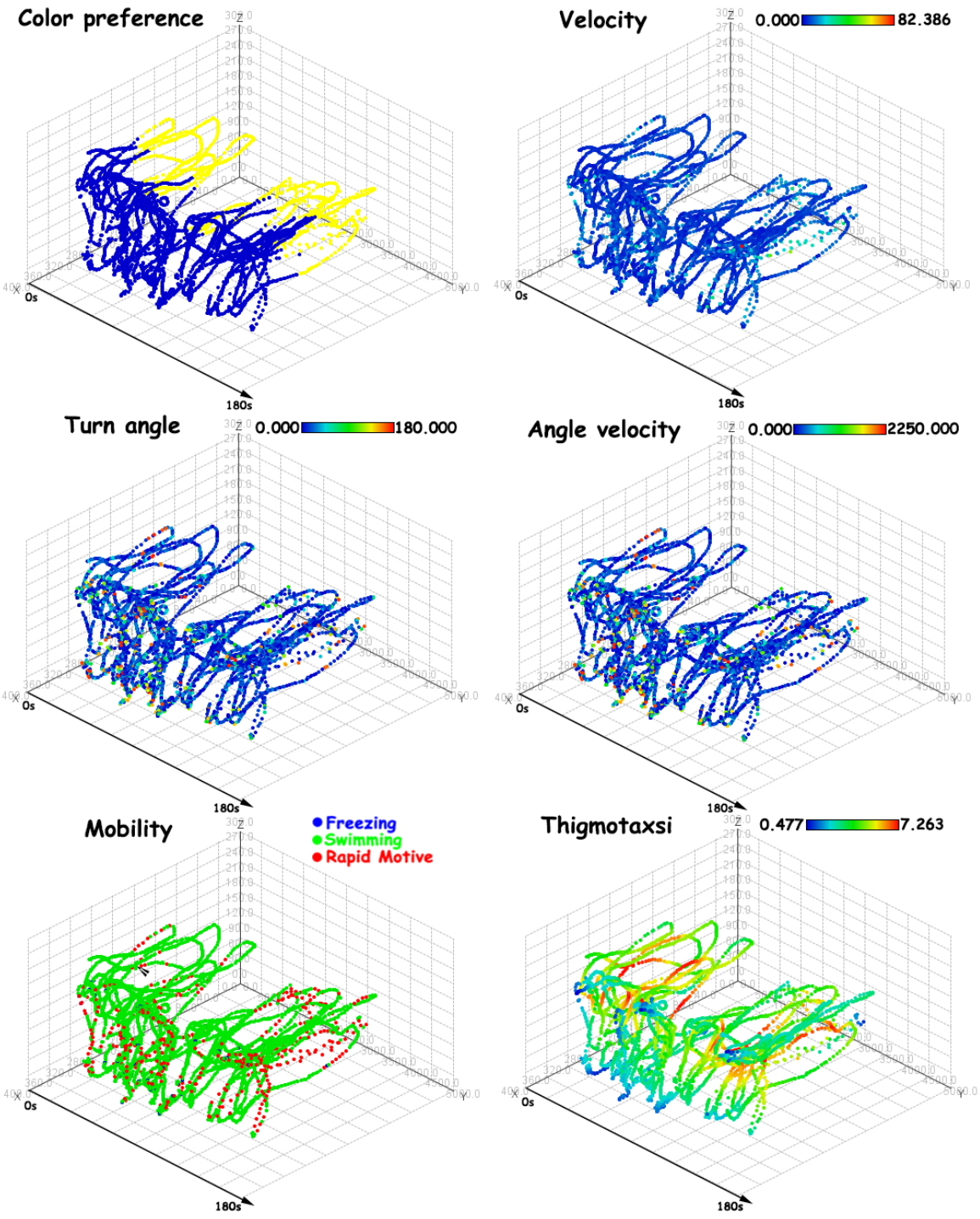

Supplementary Figure S8 (A): Wild type

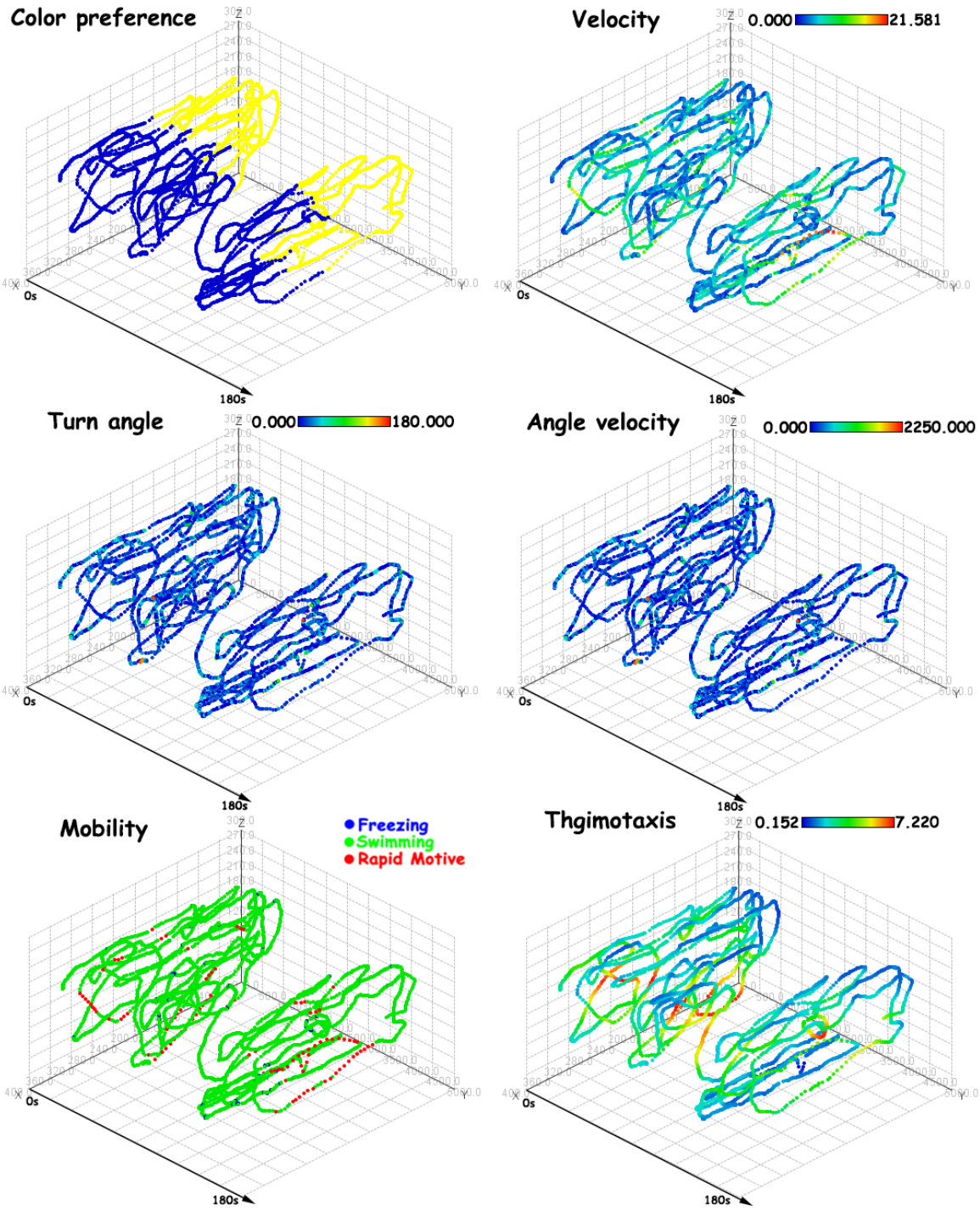

Supplementary Figure S8 (B): 50nm 300µg/mL

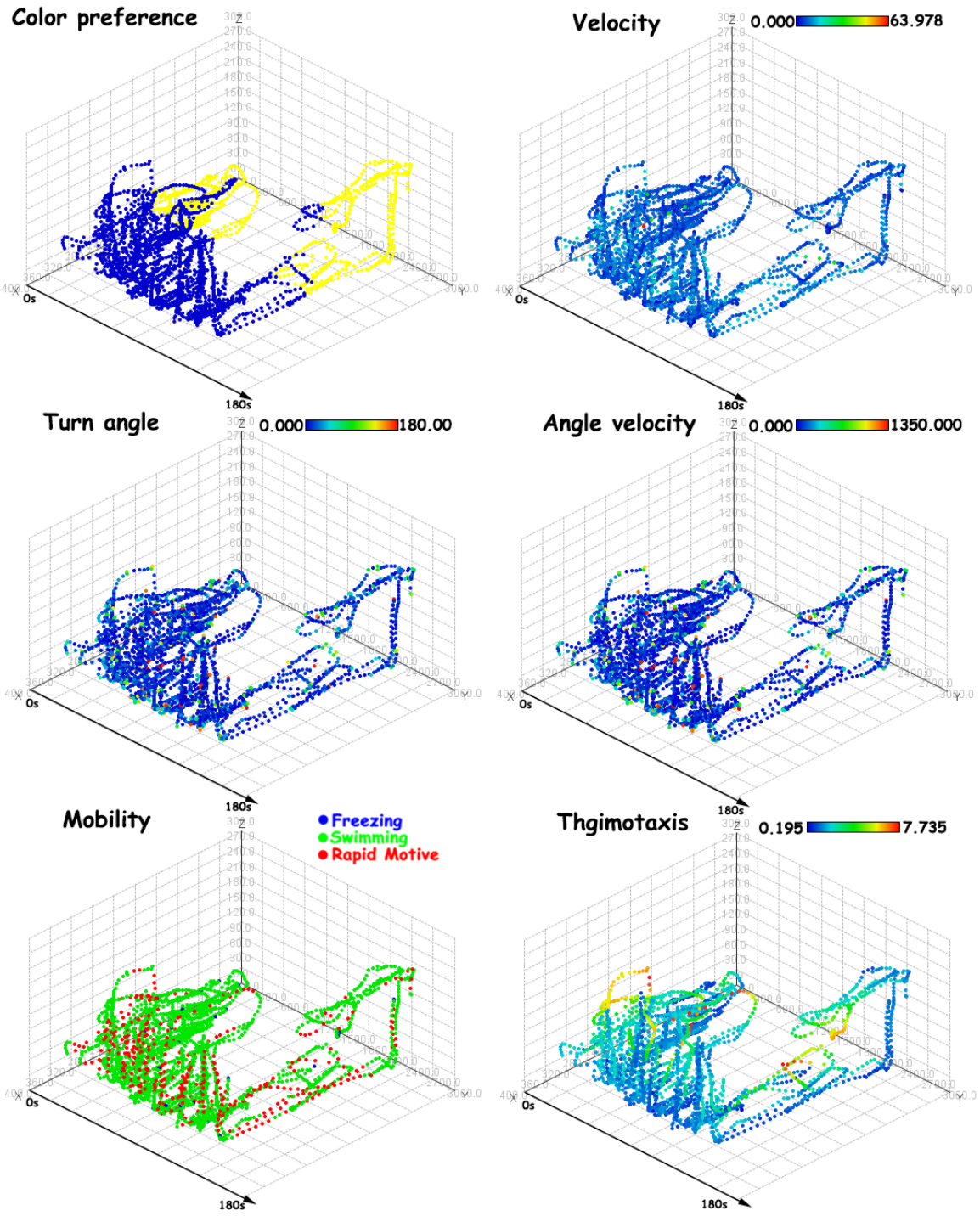

Supplementary Figure S8 (C): 50 nm 1000μg/mL

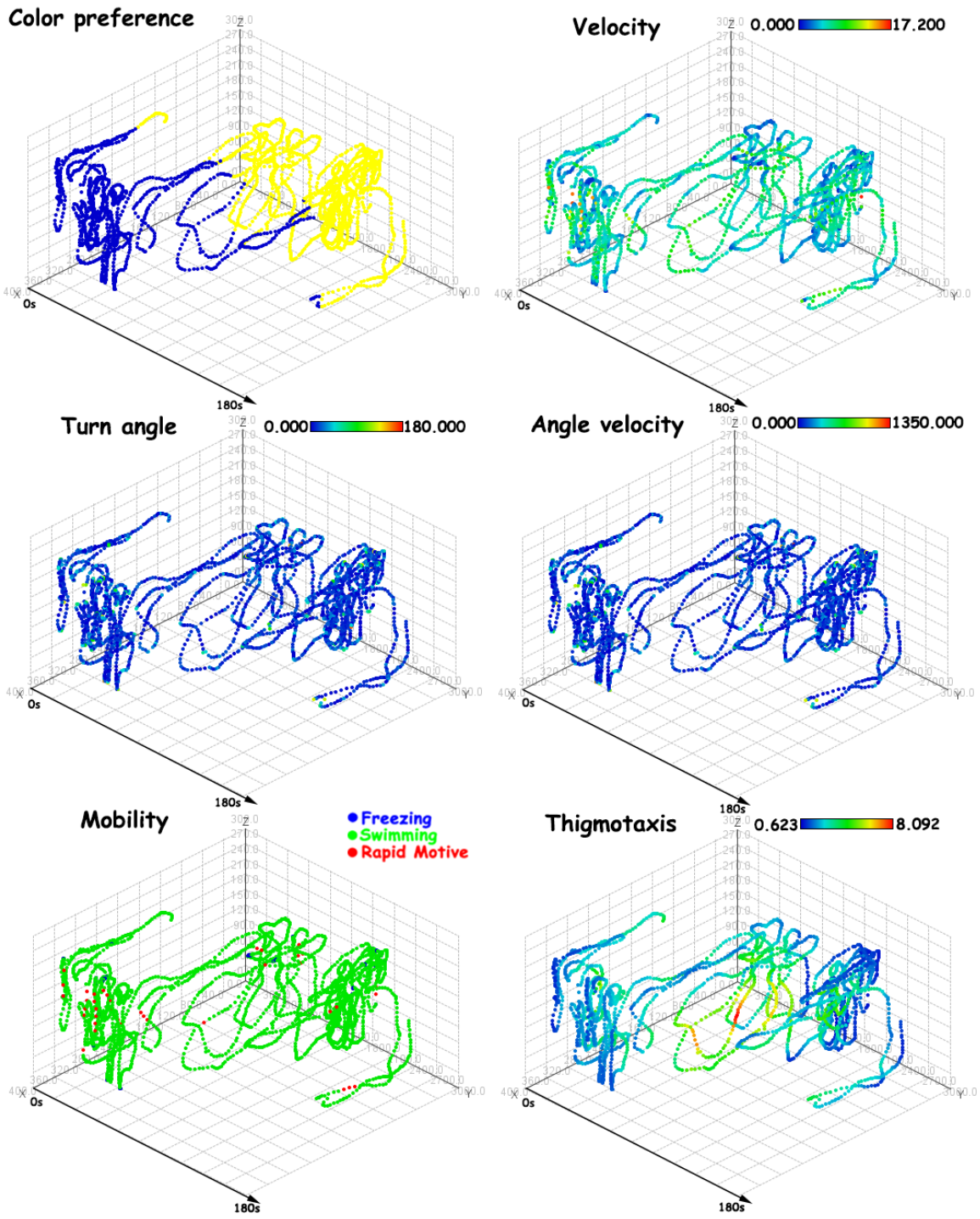

Supplementary Figure S8 (D): 15 nm 300µg/mL

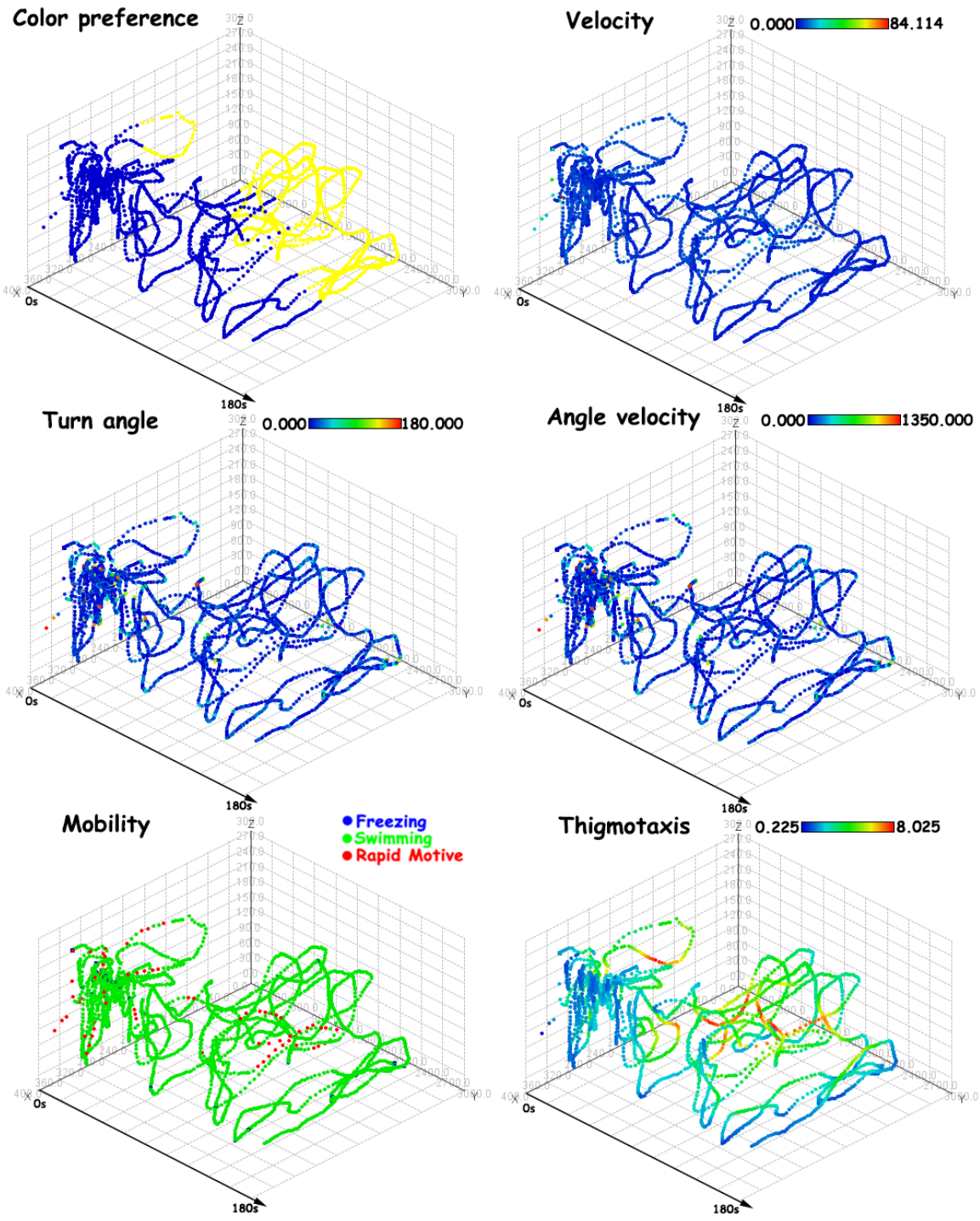

Supplementary Figure S8 (E): 15nm 1000µg/mL

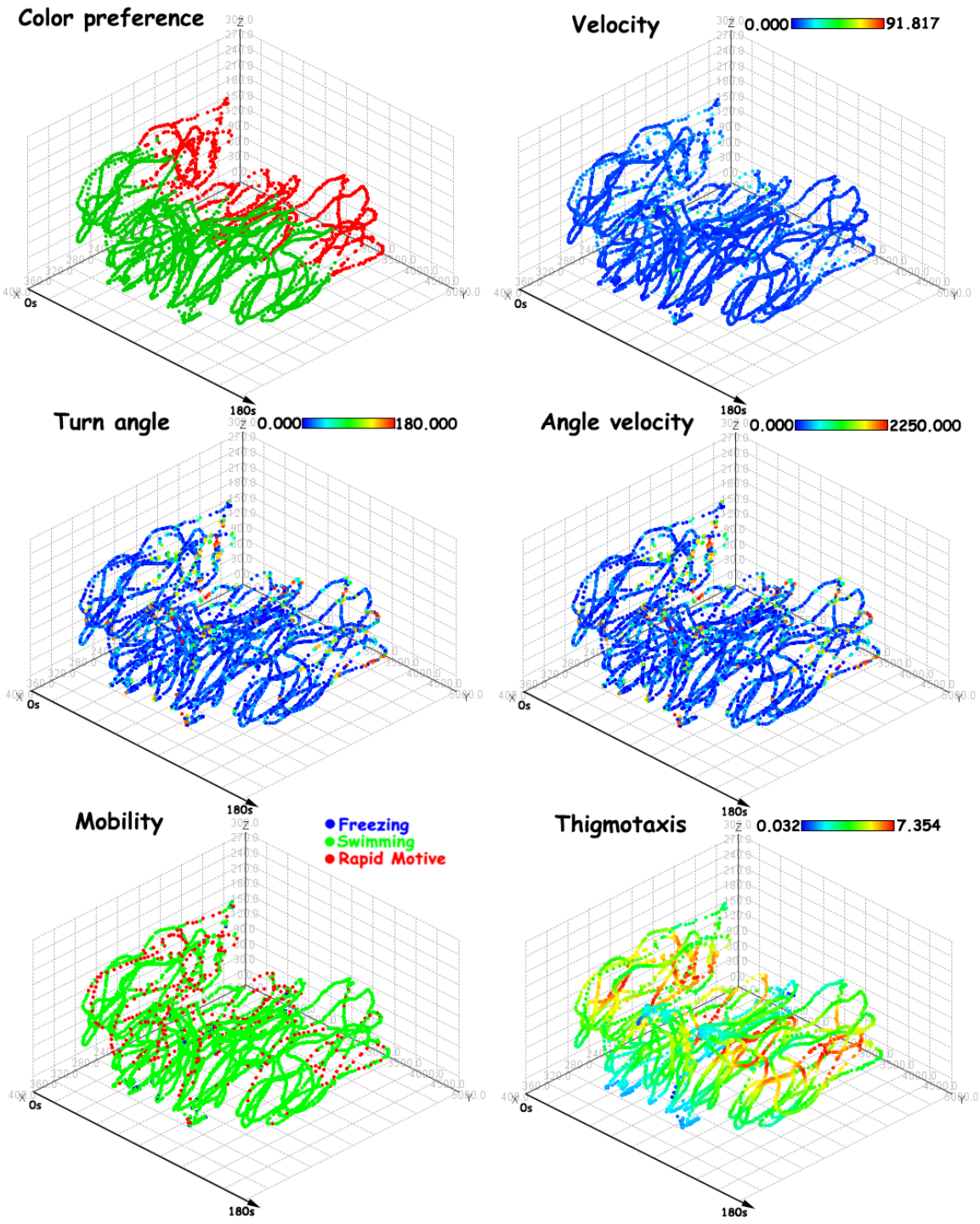

Supplementary Figure S9 (A): Wild type

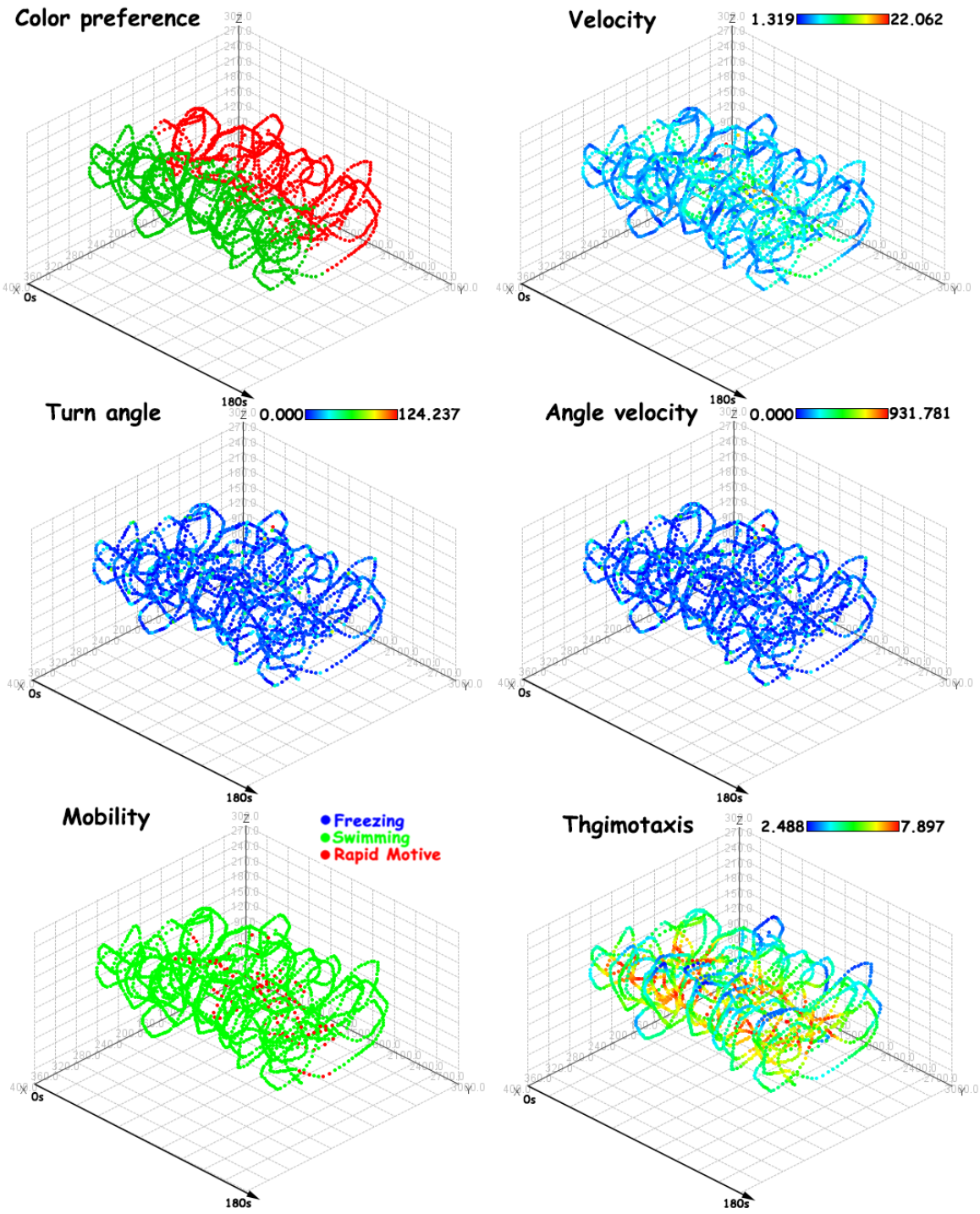

Supplementary Figure S9 (B): 50 nm 300µg/mL

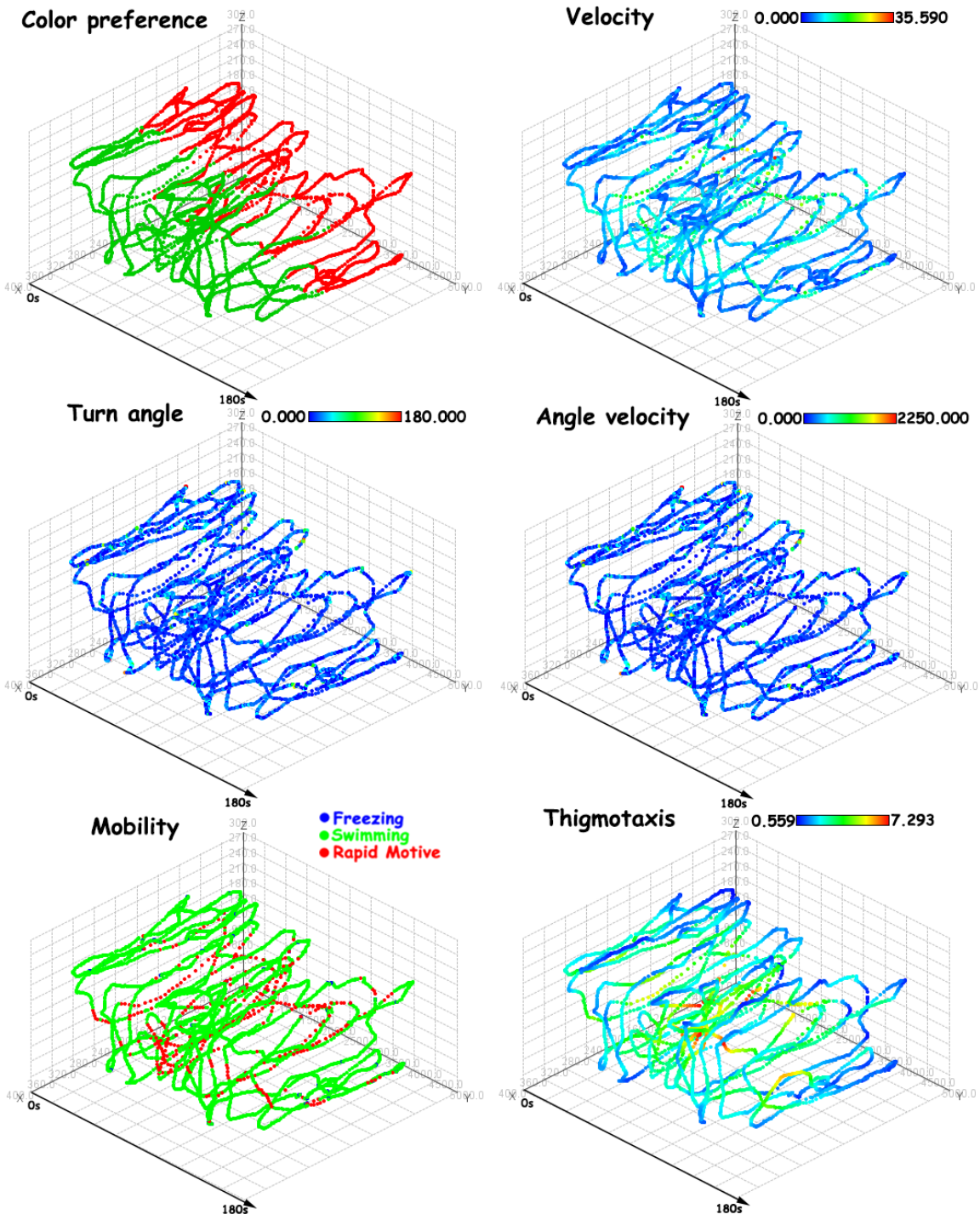

Supplementary Figure S9 (C): 50 nm 1000µg/mL

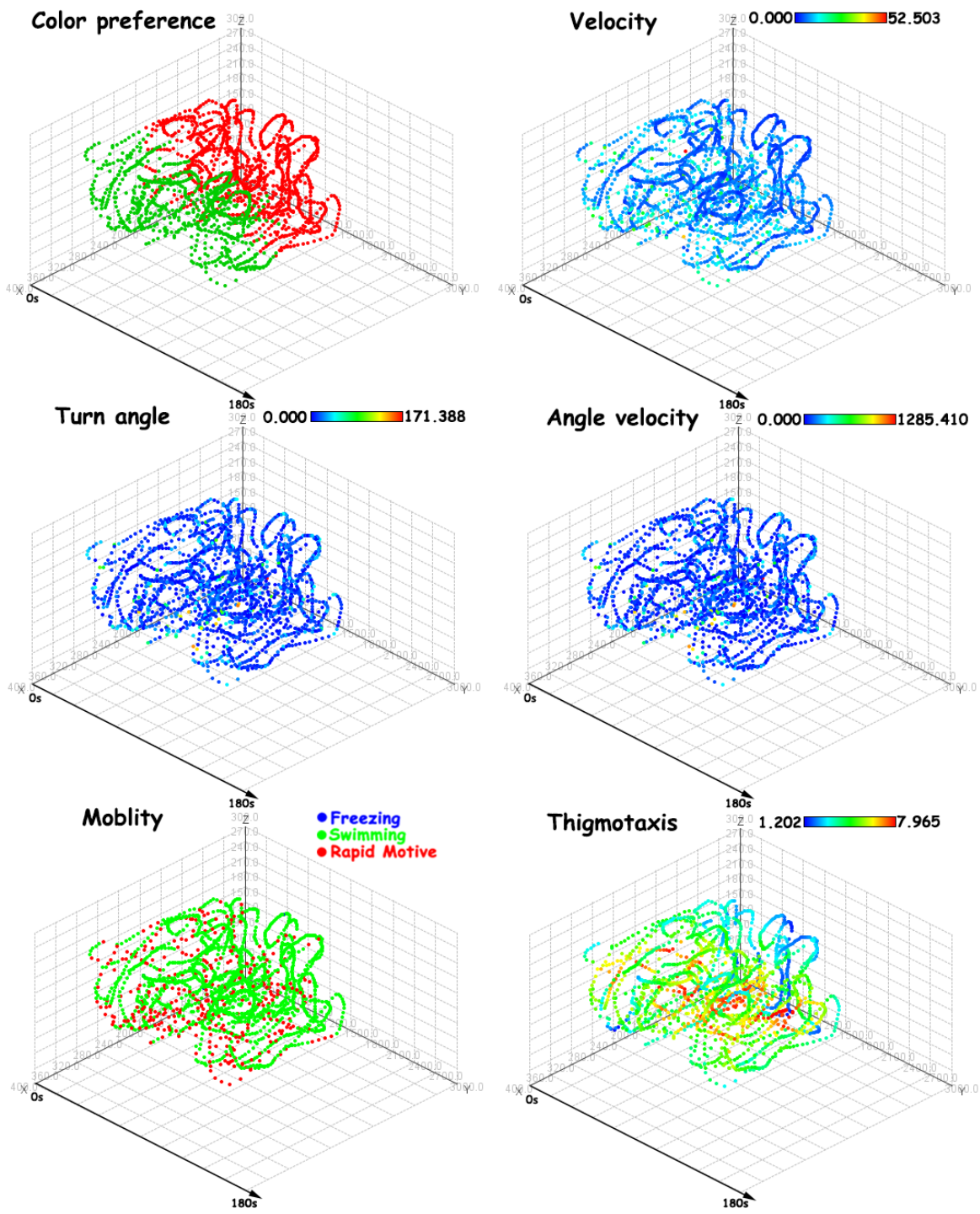

Supplementary Figure S9 (D): 15 nm 300µg/mL

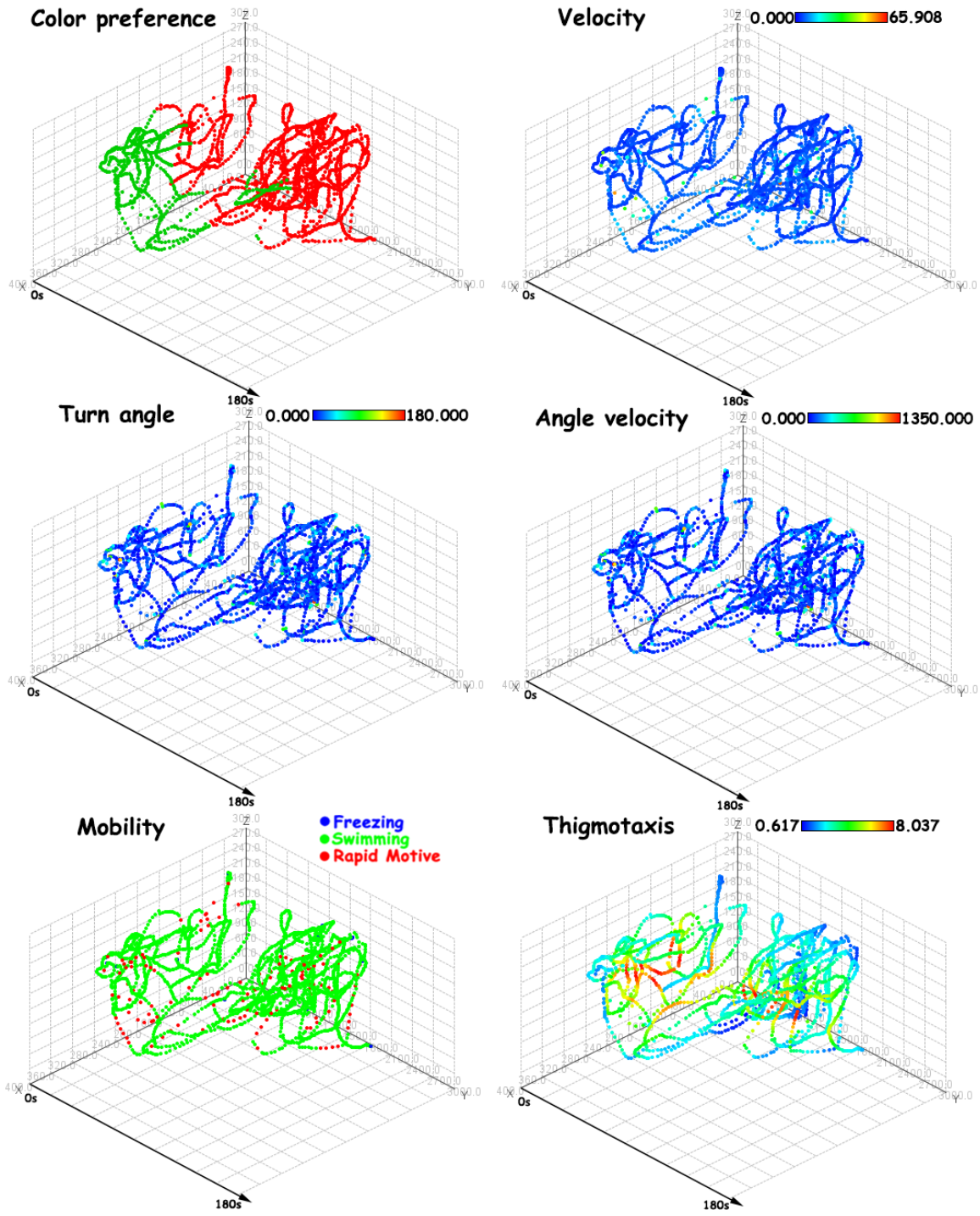

Supplementary Figure S9 (E): 15 nm 1000µg/mL

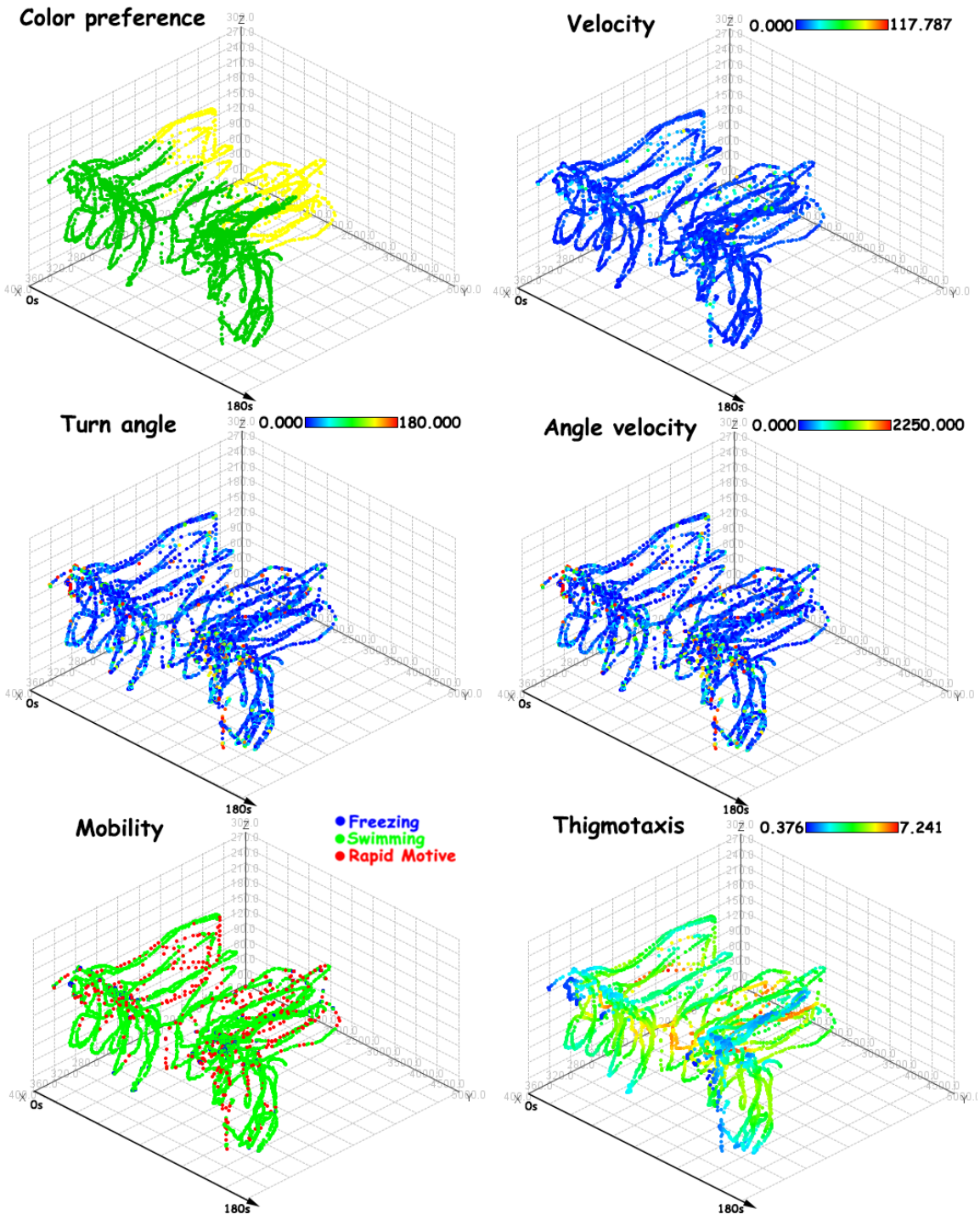

Supplementary Figure S10 (A): Wile Type

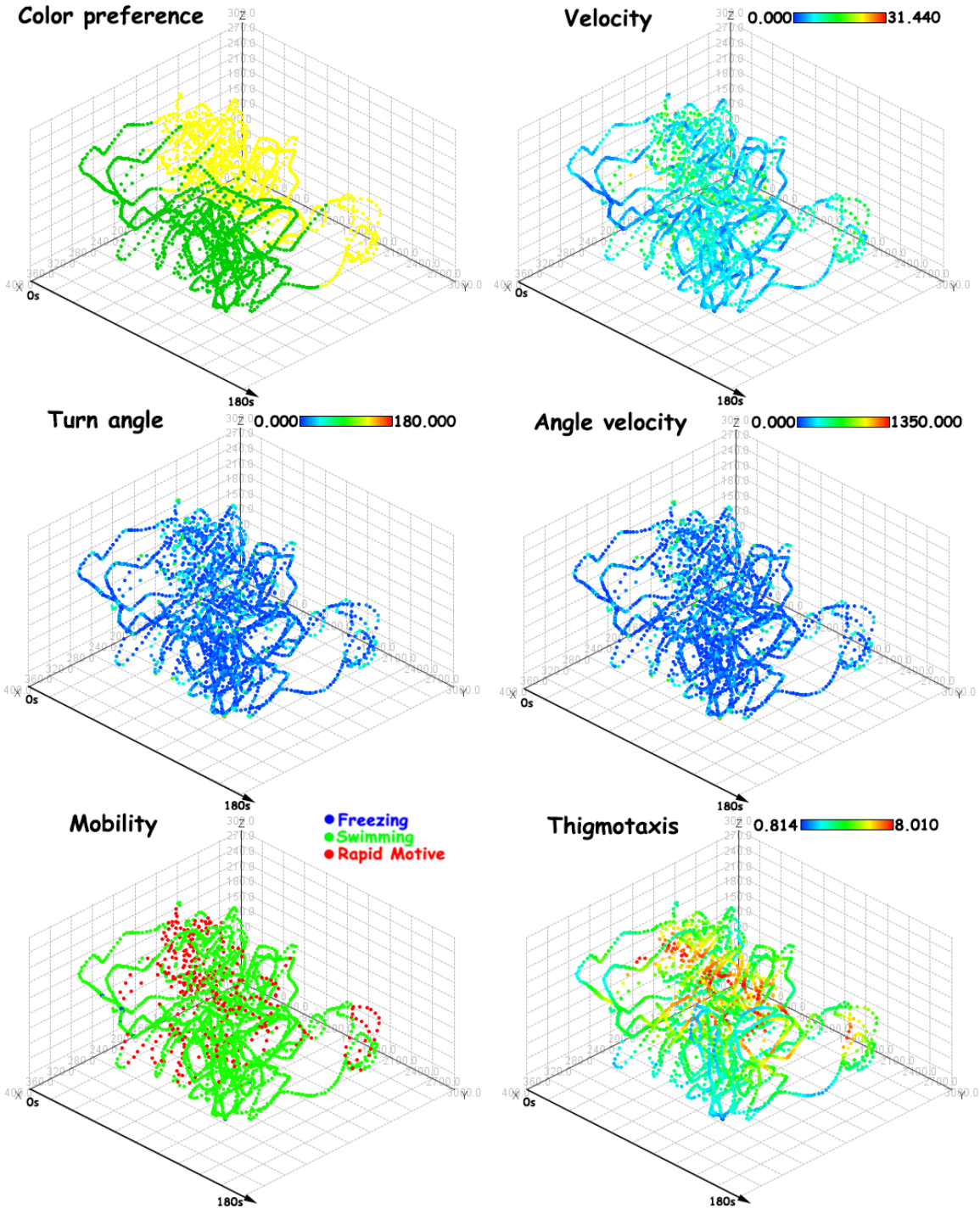

Supplementary Figure S10 (B): 50 nm 300µg/mL

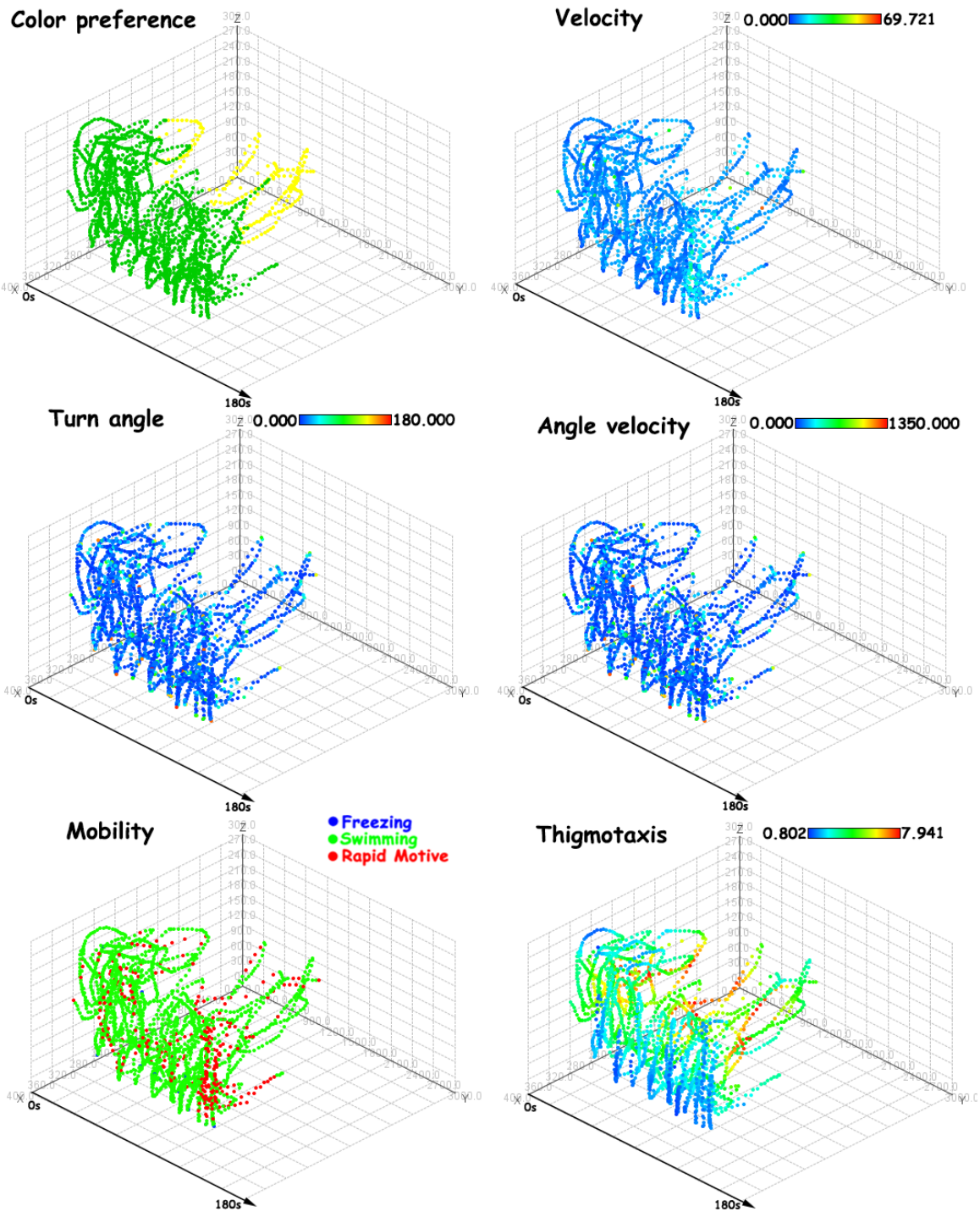

Supplementary Figure S10 (C): 50nm 1000µg/mL

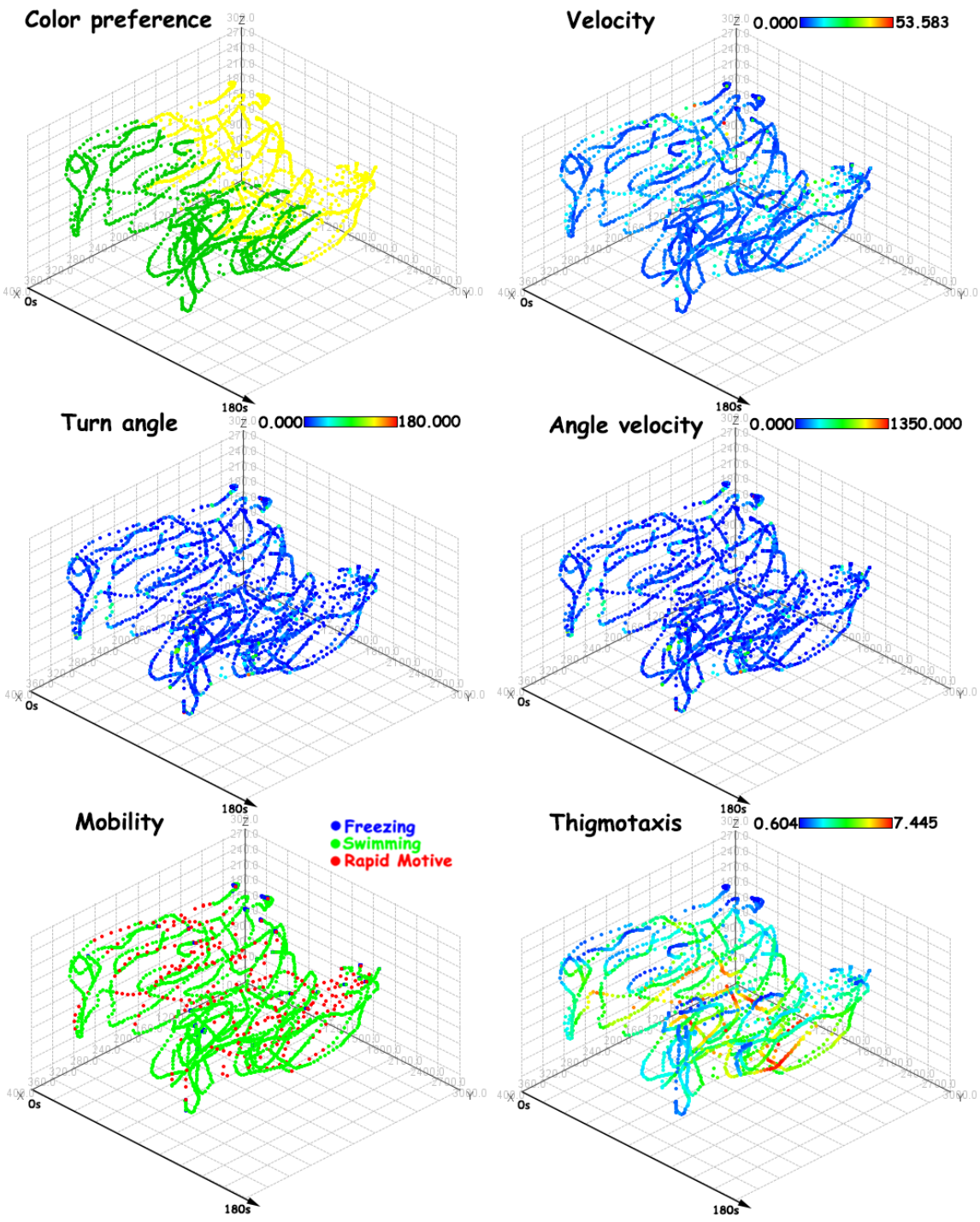

Supplementary Figure S10 (D): 15nm 300µg/mL

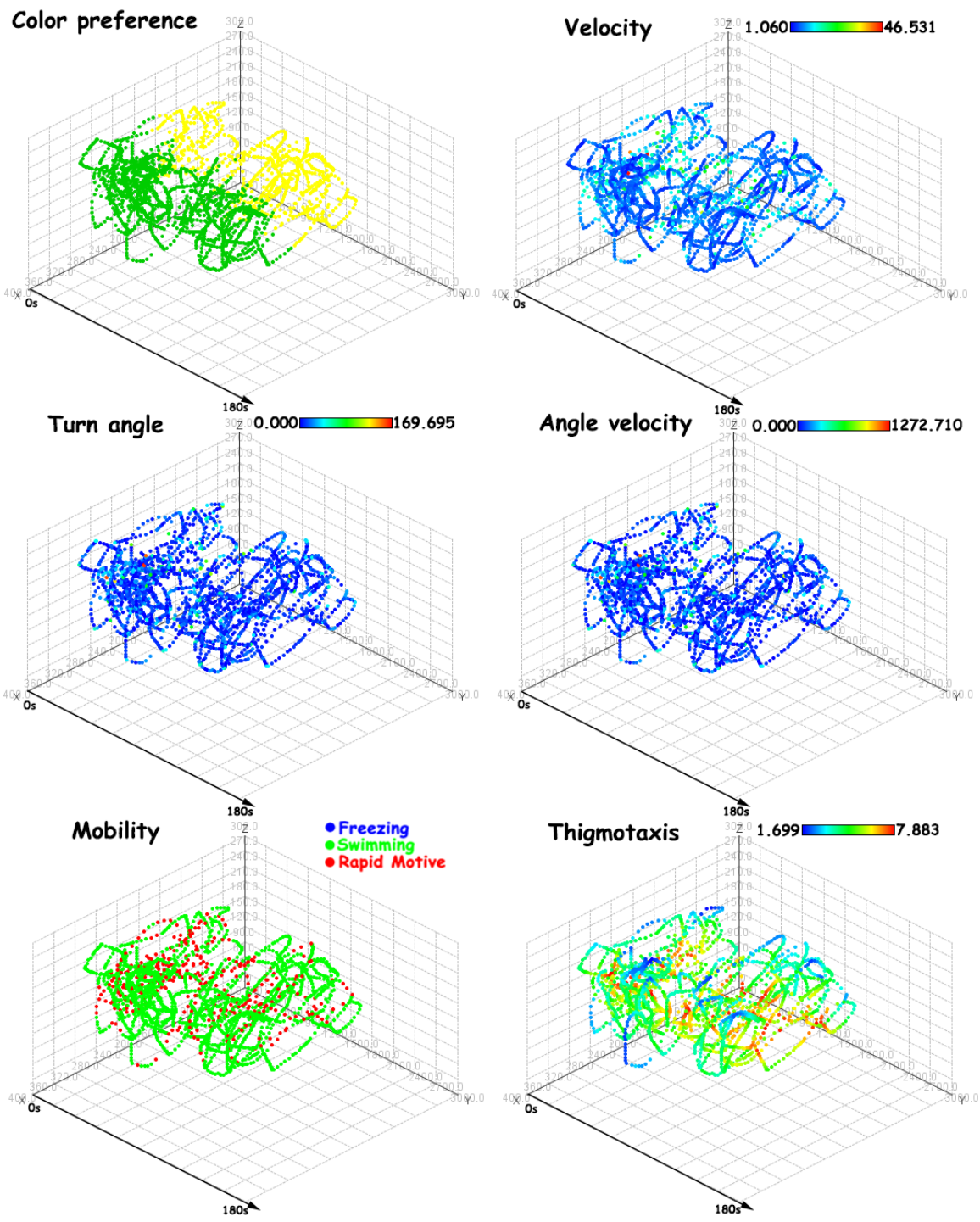

Supplementary Figure S10 (E): 15 nm 1000µg/mL

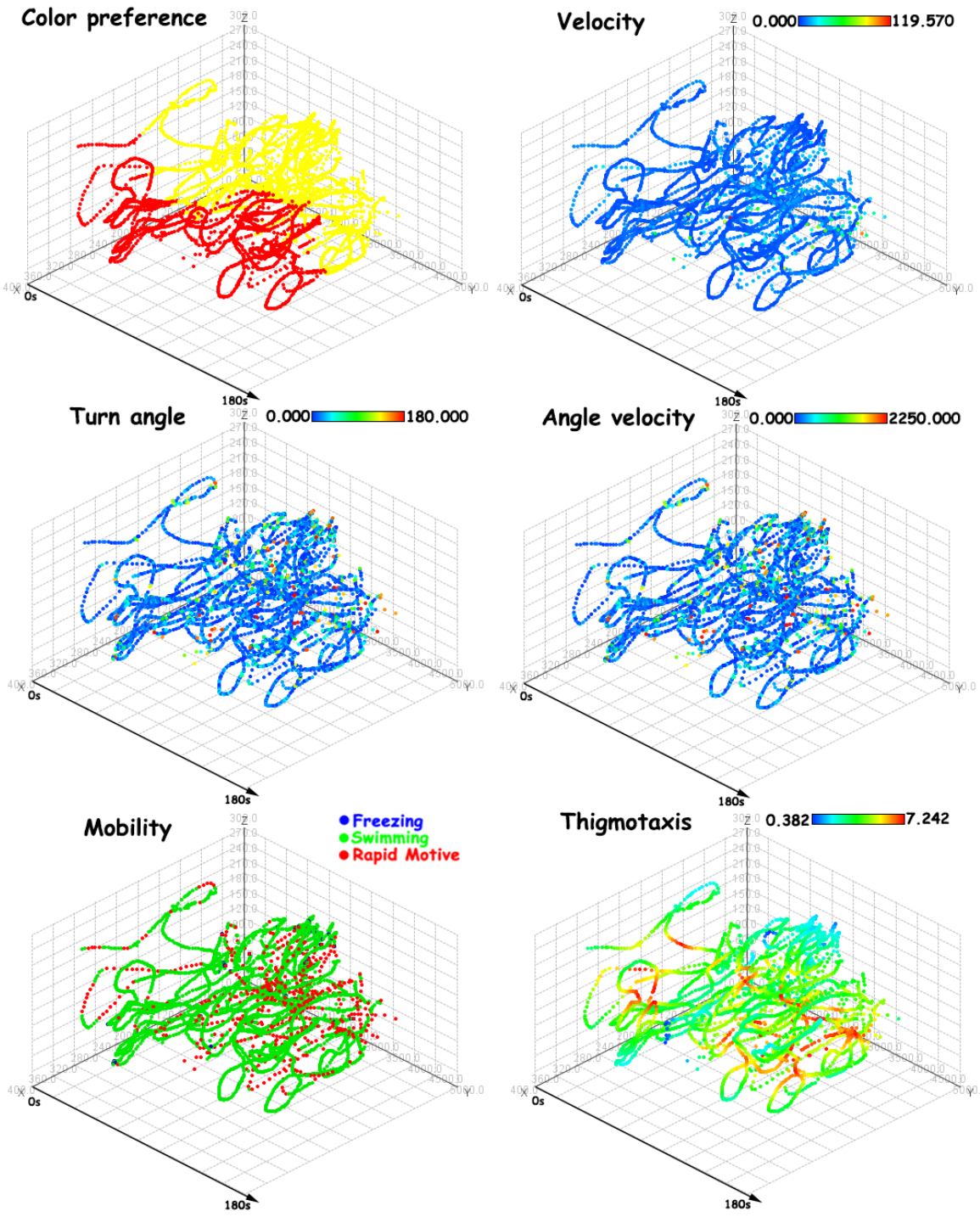

Supplementary Figure S11 (A): Wild type

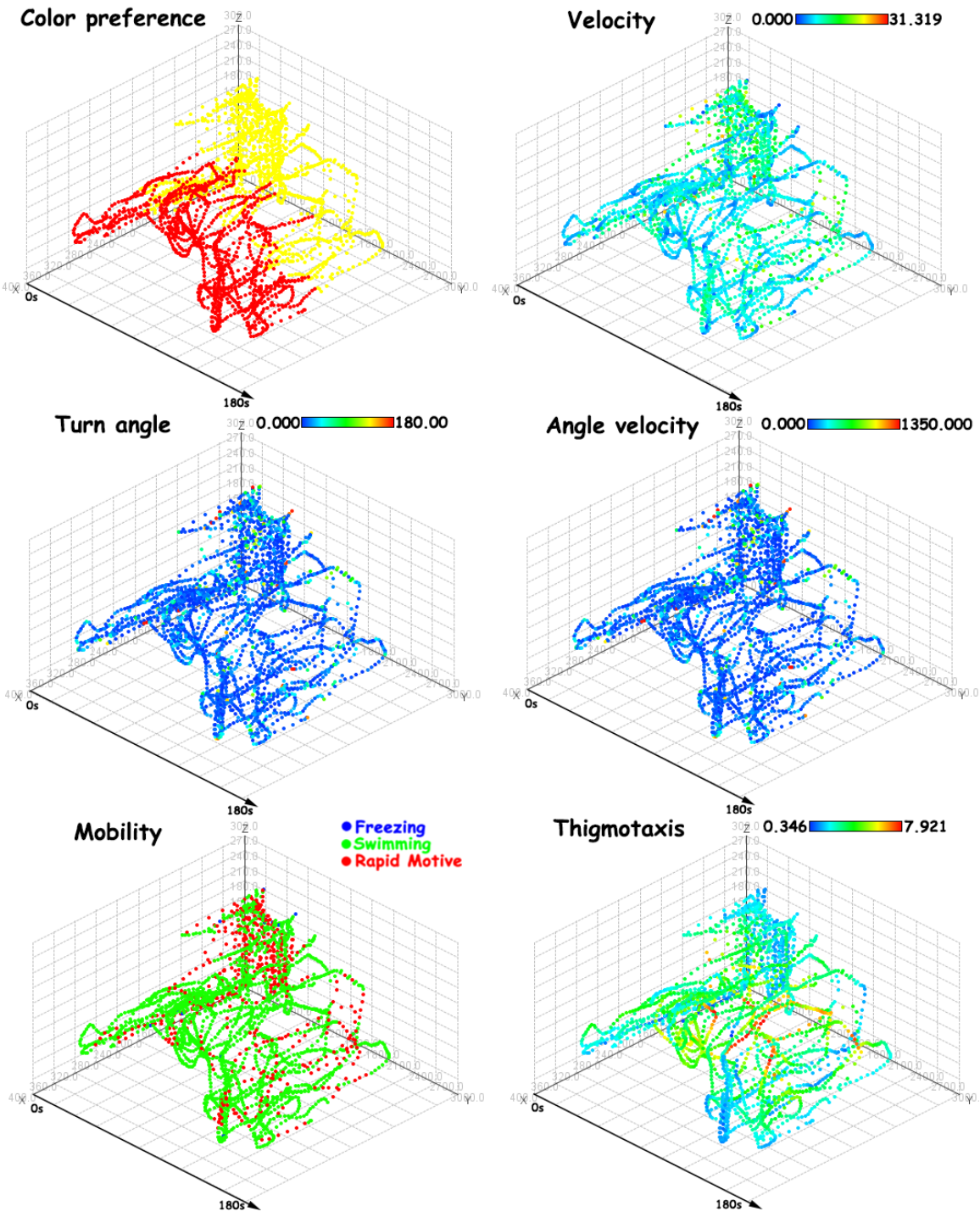

Supplementary Figure S11 (B): 50nm 300µg/mL

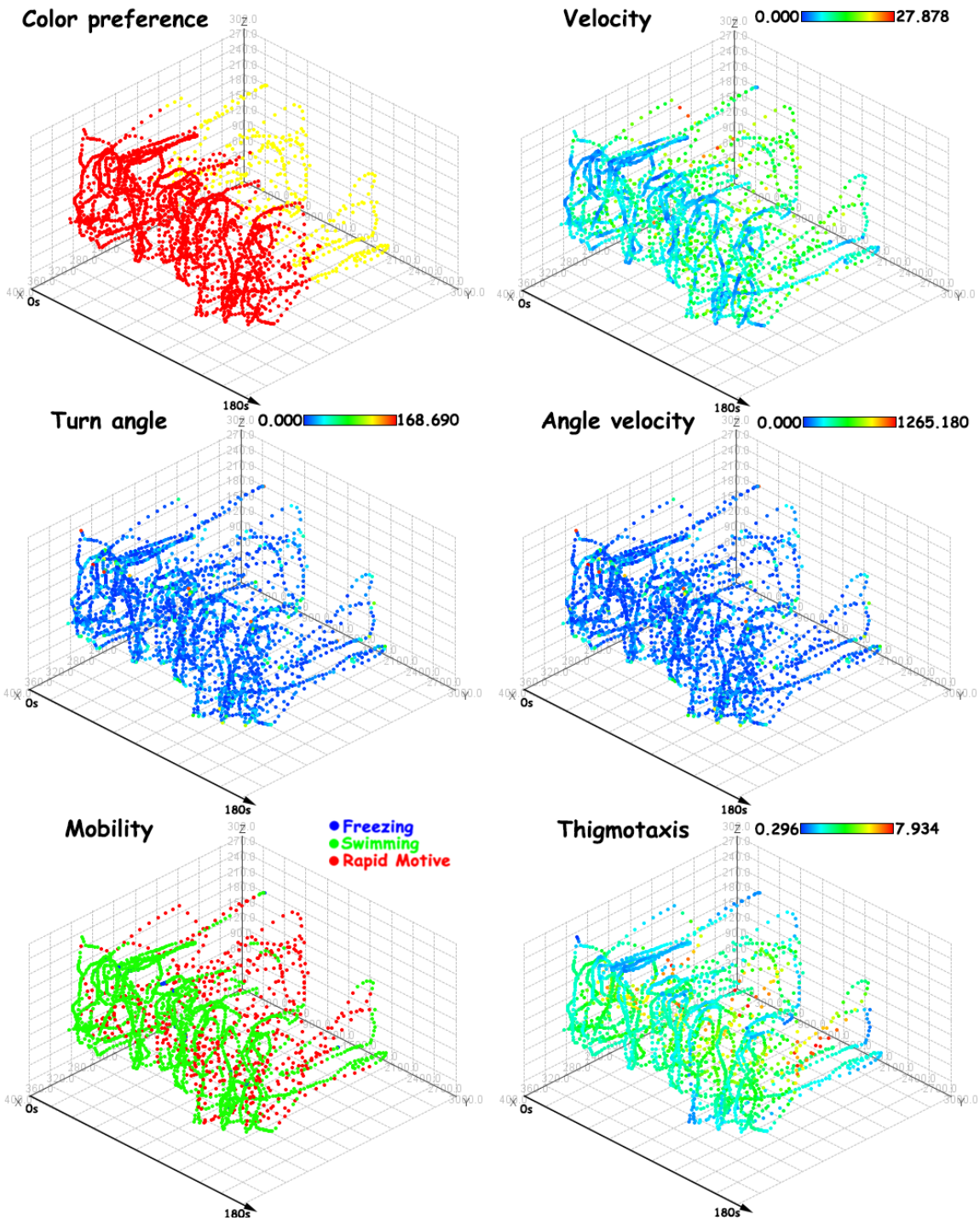

Supplementary Figure S11 (C): 50nm 1000µg/mL

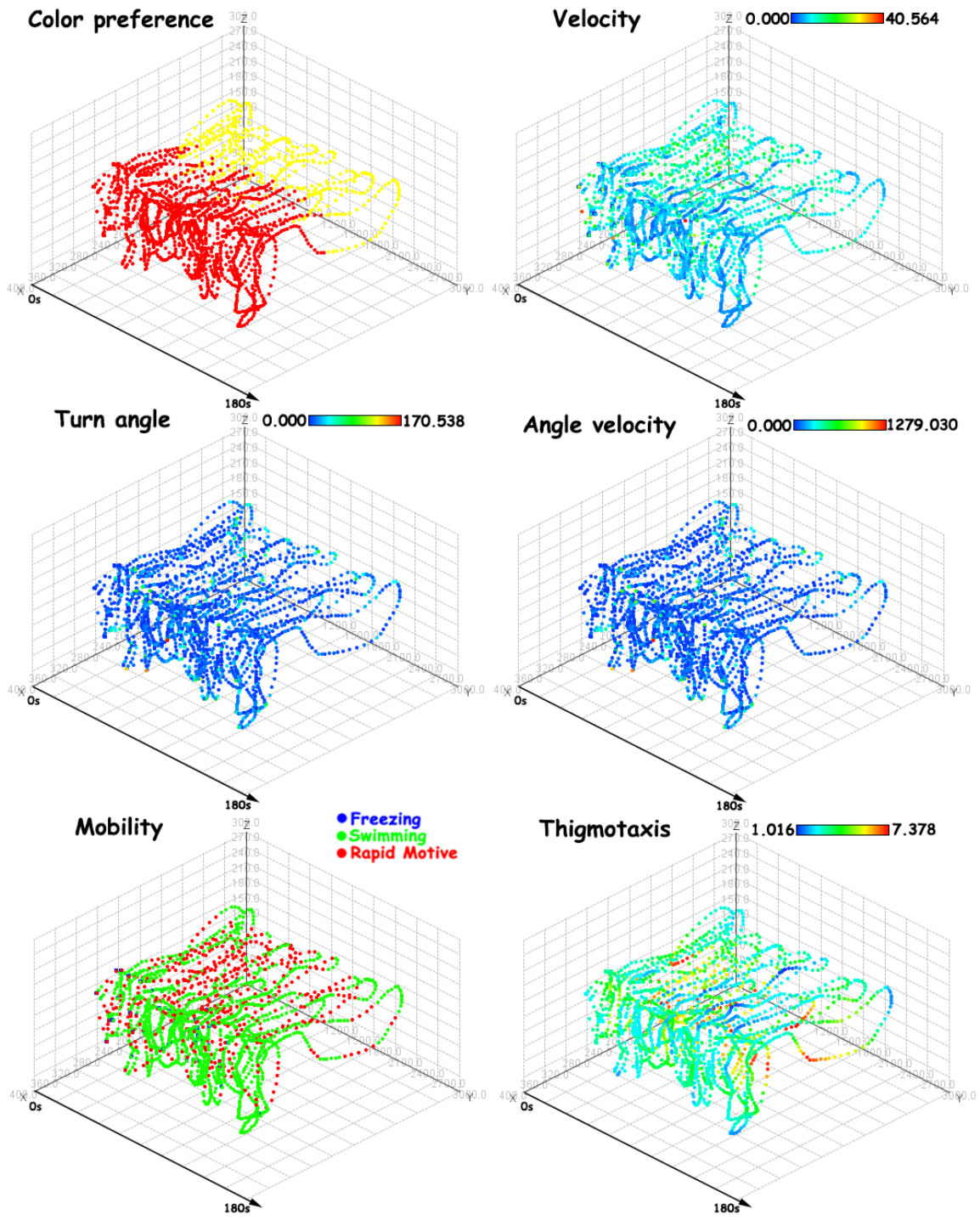

Supplementary Figure S11 (D): 15nm 300μg/mL

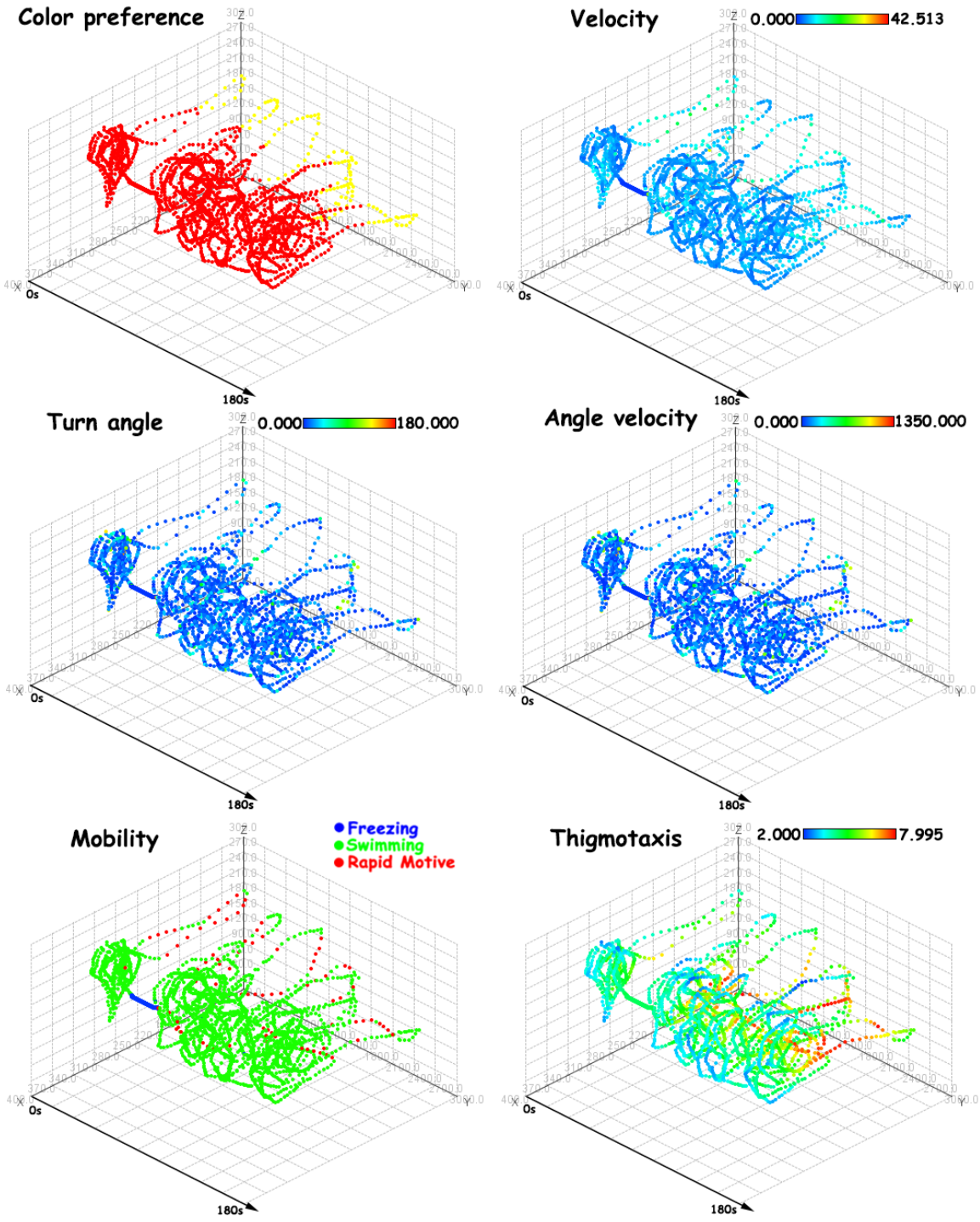

Supplementary Figure S11 (E): 15 nm 1000µg/mL

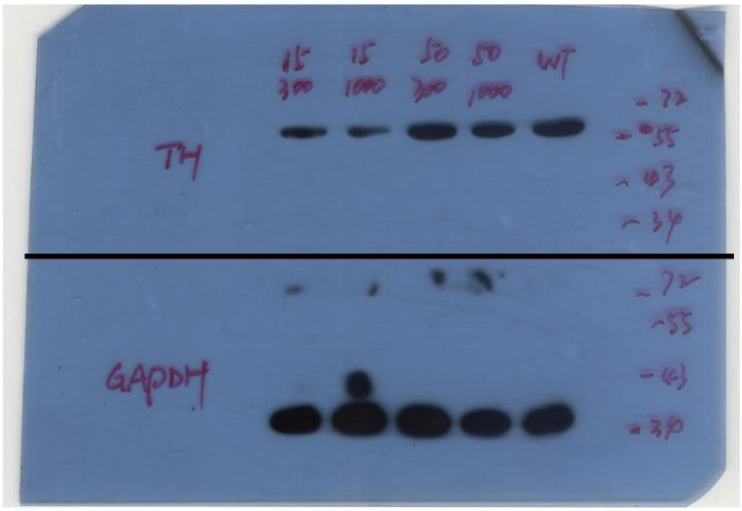

Supplementary Figure S12: Full-length blots.

SUPPLEMENTARY REFERENCE

1. Maddalena, L. & Petrosino, A. A self-organizing approach to background subtraction for visual surveillance applications. *Image Processing, IEEE Transactions* on **17**, 1168-1177 (2008).

2. Maddalena, L. & Petrosino, A. In Computer Vision and Pattern Recognition Workshops (CVPRW), *2012 IEEE Computer Society Conference* on **21-26** (IEEE, 2012).

3. Kjeldsen, R. & Kender, J. In Automatic Face and Gesture Recognition, 1996, *Proceedings of the Second International Conference* on **151-156** (IEEE, 1996).